



Hochschule für
Wirtschaft und Recht Berlin
Berlin School of Economics and Law

Master Thesis

Multi-node representational learning for classifying line item subgraphs inside order documents

Faculty 1 Economics

Department of Business and Economics

First Supervisor: Prof. Markus Löcher | markus.loecher@hwr-berlin.de

Second Supervisor: Dr. Fabian Brosig | fabian.brosig@workist.com

Berlin, July 18, 2023

By: Eger, Felix | Student ID: 890743 | Koloniestraße 31 | 13359 Berlin

Phone: 0176 31386833 | Email: felix.eger17@gmail.com

Course of Studies: M.Sc. Business Intelligence and Process Management

Statutory Declaration

I hereby formally declare that I have written the submitted Master Thesis entirely by myself without anyone else's assistance. Wherever I have drawn on literature or other sources, either in direct quotes, or in paraphrasing such material, I have given the reference to the original author or authors and to the source where it appeared. I am aware that the use of quotations, or of close paraphrasing, from books, magazines, newspapers, the internet or other sources, which are not marked as such, will be considered as an attempt at deception, and that the thesis will be graded with a fail. I have informed the examiners and the board of examiners in the case that I have submitted the dissertation, entirely or partly, for other purposes of examination.

Berlin, July 18, 2023

FELIX EGER

Abstract

Line items are integral to Table Structure Recognition (TSR) to enable automated document processing, analysis, and Business-to-Business (B2B) communications. Since Document Understanding (DU) goes beyond raw character recognition and focuses on relationships and meaning conveyed in table structures, extracting line item structures is essential. While Line Item Recognition (LIR) has predominantly been addressed with Object Detection (OD) models, little work has investigated LIR through Graph Convolutional Neural Networks (GCNs). By training two node-classification and one link-prediction model, each based on Chebyshev spectral graph convolutions, the task of assigning nodes to line items is demonstrated in this thesis. While the link-prediction task outperformed the other two, the work highlights the importance of robust node labelling methods to enable the learning of global subgraph structures on a node level.

Keywords

Graph Convolutional Neural Networks, Graph Neural Networks, Graphs, Subgraphs, Node Prediction, Link Prediction, Table Structure Recognition, Document Understanding, Line Item Recognition, Node Labeling, Order Documents, Workist

Table of Contents

1	Introduction	7
1.1	Thesis Outline	9
2	Literature Review	10
2.1	Table Understanding	10
2.2	Graphs in Information Systems	11
2.3	Graph Neural Networks	14
2.4	Graph Neural Networks in Document Understanding	19
3	Theoretical Frameworks	22
3.1	Subgraph Learning via Graph Convolutional Neural Networks	22
3.2	Node Labelling	24
3.3	Line Item Detection	26
4	Methodology	27
4.1	Data	27
4.1.1	Description	27
4.1.2	Data Pre-processing	28
4.1.3	Node Features	31
4.1.4	Edge Features	39
4.1.5	Target Labels and Training Tasks	39
4.2	Modelling Methodology	43
4.2.1	Training Methodology	43
4.2.2	Tuning Methodology	45
4.2.3	Evaluation Methodology	46
5	Artefact Description	47
5.1	Model 1: Even-Odd Prediction	47
5.2	Model 2: Link Prediction	48
5.3	Model 3: Line Item Prediction	49

6

Evaluation of Results

50

6.1

Performance on unseen Data

50

6.1.1

Model 1: Even-Odd Prediction

50

6.1.2

Model 2: Link Prediction

52

6.1.3

Model 3: Line Item Prediction

54

6.2

Ablation

56

7

Discussion and Limitations

57

8

Conclusion

64

References

65

Appendix

70

List of Figures

1	Example Document	9
2	Directed Graph	12
3	Undirected Graph	12
4	Isomorph Graph	25
5	Distribution of line item tokens	29
6	Empty Graph	30
7	All Tokens	30
8	Only Line Item Tokens	30
9	Single Line Item	30
10	Node Colouring approach	38
11	Distribution of even-odd labels	41
12	Single Token comparison	41
13	Single Token comparison within neighborhood context	42
14	Parallel Coordinates Plot, Even-odd Prediction	48
15	Parameter Importance, Even-odd Prediction	48
16	Parallel Coordinates Plot, Link Prediction	49
17	Parameter Importance, Link Prediction	49
18	Clustering Results, Even Line Items, Example 1	58
19	Clustering Results, Odd Line Items, Example 1	59
20	Clustering Results, Even Line Items, Example 2	59
21	Clustering Results, Odd Line Items, Example 2	60
22	Example Document of left token	74
23	Example Document of right token	75
24	Easy document graph	76
25	Medium document graph	77
26	Hard document graph	78
27	Link prediction inference, Example 1	79
28	Link prediction inference, Example 2	80

29	Even-odd inference, Example 1	81
30	Even-odd inference, Example 2	82

List of Tables

1	Adjacency Matrix	13
2	Degree Matrix	13
3	Parameter ranges of tuning	45
4	Performance, Even-odd Prediction	51
4	Performance, Even-odd Prediction	52
5	Results per target, Even-odd Prediction	52
6	Performance, Link Prediction	53
6	Performance, Link Prediction	54
7	Results per target, Link Prediction	54
8	Performance, Line-item prediction	55
9	Ablation Study, Even-Odd Prediction	56
10	Ablation Study, Link Prediction	57
11	Performance, Pipeline approach	60
12	Tuning Results, Straight-odd Prediction	70
12	Tuning Results, Straight-odd Prediction	71
13	Tuning Results, Link Prediction	71
13	Tuning Results, Link Prediction	72
13	Tuning Results, Link Prediction	73

List of Acronyms

B2B Business-to-Business. 3, 7, 8, 27, 28

BFS Breadth-First Search. 14

CNN Convolutional Neural Network. 15, 16, 19, 20

CS Computer Science. 11

CV Computer Vision. 7

DBSCAN Density-Based Spatial Clustering of Application with Noise. 59, 60

DFS Depth First Search. 14

DL Deep Learning. 10, 63

DU Document Understanding. 3, 7, 22, 65

ERP Enterprise-Resource Planning system. 10, 21, 27

GAT Graph Attention Network. 18, 19

GCN Graph Convolutional Neural Network. 3, 8, 9, 15–20, 26, 28, 39, 43

GFT Graph Fourier Transform. 16

GNN Graph Neural Network. 8–10, 14, 19, 20, 23, 24, 26

IDP Intelligent Document Processing. 7

KNN K nearest neighbor. 20

LIR Line Item Recognition. 3, 8, 65

LSTM Long-Short Term Memory Network. 14, 17, 19, 20

ML Machine Learning. 7, 11

NLP Natural Language Processing. 7

OCR Optical Character Recognition. 7, 21, 28, 30

OD Object Detection. 3, 10, 11, 26, 28, 62

R-CNN Recurrent Convolutional Neural Network. 19

RELU Rectified linear Unit. 15, 18

RNN Recurrent Neural Network. 14

SME Small-to-Medium-sized Enterprises. 27

TC Table Classification. 11

TD Table Detection. 10, 11

TSR Table Structure Recognition. 3, 7, 11, 65

TU Table Understanding. 10

1 Introduction

Document Understanding (DU) and Intelligent Document Processing (IDP) is an active field of research that combines a multitude of disciplines, such as Machine Learning (ML), Natural Language Processing (NLP), and Computer Vision (CV). Vashisth et al., 2022 explain that the solutions developed in this area target extracting textual data inside documents for analysis and workflow automation. As Šimsa et al., 2023 show, Business-to-Business (B2B) communications rely on exchanging documents, such as invoices or orders, and consequently require substantial manual data entry to process the document information. Consequently, the market and research for IDP solutions has been growing significantly in recent years and was estimated by Vashisth et al., 2022 to reach \$4.8 billion by 2022.

Optical Character Recognition (OCR), such as Smith, 2007, can recognize and locate characters in an image. While OCR solutions are necessary to extract information from a document, IDP solutions' automatic extraction and processing of documents goes beyond raw character recognition. To understand written content, using NLP methods, such as Devlin et al., 2018 has proven to improve the understanding of natural language. Moreover, the detection of specific objects in documents, such as tables, headers, or line items, is performed by object detection models, such as Šimsa et al., 2023, Schreiber et al., 2017 or Smock et al., 2022. Since information inside a document is also contained through its layout, format, and the mixture of graphical elements such as images or tables, information inside a document is also captured through the structure. Moreover, Aiello et al., 2002, and Šimsa et al., 2023 explain that authors follow a logical ordering and arrange information accordingly, thus capturing relational information in the hierarchical arrangement of elements. Therefore, extracting and understanding the structure can provide useful information regarding the relation and role of an element in a document. Specifically, the task of Table Structure Recognition (TSR) deals with understanding the structural organization of tables and their physical and logical content, as defined by Coüasnon and Lemaitre, 2014. Since tables inside B2B documents contain vital information, extracting the content and its arrangement plays an important role in downstream processing tasks. Inside order documents, invoices, and delivery notes, line items are a structural component of tables that describe an isolated logical unit of an order line. Identifying line items and assigning table elements to each line item is the scope of this thesis.

There have been numerous attempts in research to detect tables and even line items through object

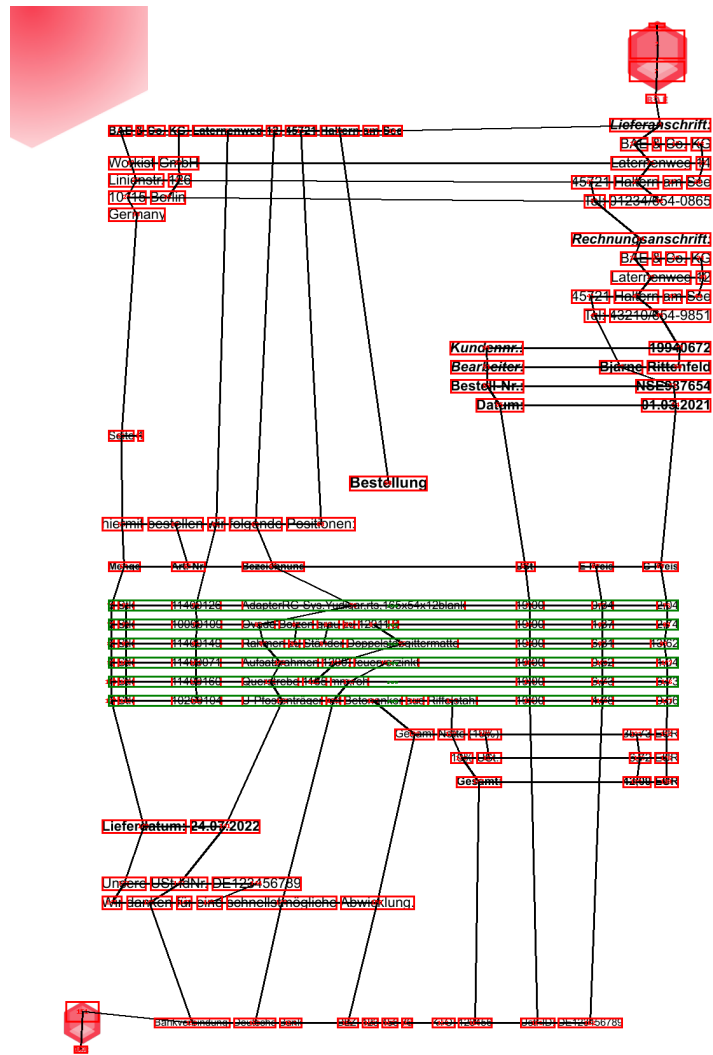
detection models, such as Šimsa et al., 2023, Schreiber et al., 2017 or Smock et al., 2022. While each of the papers successfully detected tables or line items, they only identified the area in a document in which the object is contained. However, since line items represent different aspects of an order, such as article number, price, or quantity, the individual values of each line item element are not represented in object detection models. As an alternative to object detection models, B2B documents have been processed through the use of graph models, as shown by Riba et al., 2019, Qasim et al., 2019, Holeček et al., 2019, Lohani et al., 2019, or Chi et al., 2019. Despite each paper having a different prediction task, they use graphs as a modelling tool to represent individual document elements, tokens, and their relation. However, none of the papers explicitly used Graph Neural Networks (GNNs) to classify line items directly. The task of identifying line item structures using GNNs is thus relatively unexamined. Documents are represented as graphs to capture the relationship between individual tokens and to identify line items. An example representation of an order document including tokens and their relationship is shown in Figure 1. The challenge lies in assigning tokens inside the document to a specific line item. To challenge this task, the question leading this paper is formulated as:

RQ: *“How can the architecture of Graph Neural Networks be modified to classify line item subgraph structures inside order documents?”*

In this work, three different approaches are used to classify line items. First, nodes are predicted to be on an even or odd line item. Second, the edge between tokens on the same line item is predicted, and lastly, the line item number is predicted per node. For each training task, separate models are trained and evaluated on a test set. The task of learning line item structures is shown to be feasible using Graph Convolutional Neural Networks (GCNs), while the link prediction task performs best. Moreover, the work highlights the importance of node labelling to generate informative node representations.

This thesis contributes to demonstrating Line Item Recognition (LIR) by utilising GCNs for node classification and link prediction. It provides a novel approach to identifying line items by expanding existing automated data extraction techniques. Furthermore, it highlights the importance of efficient node labelling techniques to enable subgraph learning for node-level representations.

Figure 1: Example Document



Red rectangles indicate bounding boxes around tokens

Green rectangles indicate bounding boxes around line items

1.1 Thesis Outline

The theoretical foundations discussed in the following chapter will provide a deeper understanding of the field of DU, the task addressed, and the model infrastructure used. The Chapter, Theoretical Frameworks, expands on the introduction to GNNs and GCNs and focuses on critical parts of the implemented model and specific research dealing with graph models in DU. Chapter 4 explains the data used for training, the pre-processing and engineering, and the methodology used for training. Chapter 5 describes the artefacts generated through this study. Following Chapter 5, the model performance is evaluated on unseen test data and feature importance analyzed via an ablation study. The

results and implications are reviewed and discussed in Chapter 7.

2 Literature Review

This chapter aims to give an overview of the research in GNN in recent years, the domain of Table Understanding (TU), and its combination. At first, the field of TU, necessary prior research, and definitions are explained. The following chapter reviews the data structure of graphs and its potentials and limitations for Deep Learning (DL). Subsequently, the development of GNNs is explained while focusing on critical historical discoveries and recent advancements. Finally, specific papers dealing with table and document extraction based on graph models are reviewed and evaluated.

2.1 Table Understanding

Inside documents, tables present a structured information organization and contain data with some form of logical connection in a horizontal or vertical domain. As defined by Costa e Silva et al., 2006, tables are a graphical grid-like matrix M_{ij} , where:

1. each element i, j of the matrix is atomic
2. there exist linear visual clues, meaning the elements in each row tend to be horizontally aligned
3. linear visual clues describe logical information
4. eventual line art does not add meaning that is not available otherwise

As motivated by the same paper, companies worldwide must process structured documents, such as financial reports. This process can be extended to other departments that process administrative documents, such as Procurement, Legal, or Sales. In Procurement documents, such as invoices, order documents, or delivery notes, tables contain highly relevant information that needs further processing through an Enterprise-Resource Planning system (ERP). As defined by Coüasnon and Lemaitre, 2014, table processing can roughly be split into three main categories: detection, classification, and recognition. The order of these different tasks expands in difficulty.

Coüasnon and Lemaitre, 2014 explain that Table Detection (TD) deals with identifying if a table is present in the document and, if yes, where it is placed. Various approaches have been dealing with TD, such as Riba et al., 2019, Schreiber et al., 2017, and Shafait and Smith, 2010. At the time of writing, Object Detection (OD) models such as Schreiber et al., 2017, Smock et al., 2022, and Prasad

et al., 2020, are most prominently used for TD.

Table Classification (TC), on the other hand, deals with the task of assigning each table or object in a document to a pre-defined class. While it is less common to classify tables as a whole, some papers deal with classifying table headers, such as Fang et al., 2012.

Finally, TSR aims to extract the table's content and infer the function of elements inside the table. Coüasnon and Lemaitre, 2014 explain that apart from recognising the logical content, the structure of a table must also be recognised. The focus of this thesis can be classified as being part of TSR since it deals with the classification of line items, a particular set of table structures. Compared to research on TSR based on OD, tables are represented as graphs, as shown in Figure 1. This representation means that each table and its content are considered individual objects with some form of relation to each other instead of an image of the document to infer its structure. While this approach has the advantage of directly representing document tokens in the model, it does incorporate some drawbacks for processing graphs as an input data structure. The following chapter explains graphs in Computer Science (CS) and their complexity as an input source for ML.

2.2 Graphs in Information Systems

Graphs in CS present a flexible modelling tool, able to capture the relationship between entities and can thus be applied to various tasks. In the focus of this paper, graphs are used as a data structure. As Singh and Sharma, 2012 explain, graphs used as a data structure must be rich enough to mirror the underlying relationships, and their structure should be simple enough for processing. Both criteria are fulfilled in the application of graphs to the problem of this thesis.

Majeed and Rauf, 2020 formally denote a graph G as $G = (N, E)$, where N is a set of nodes, and E is a set of vertices connecting the nodes. Graphs can either be directed or undirected, implicating a direction between nodes or no direction. An undirected graph can be understood as a directed graph with two edges between each pair of nodes in both directions. An example directed graph is shown in Figure 2, in which arrows indicate the direction, and an undirected graph is shown in Figure 3.

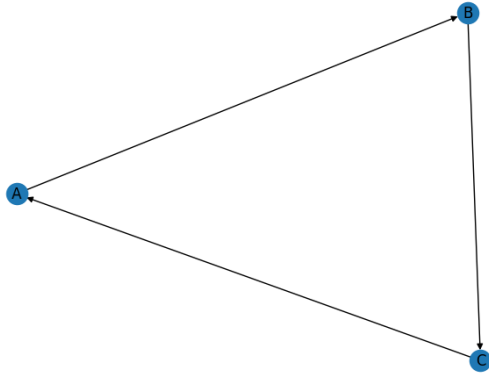


Figure 2: Directed Graph

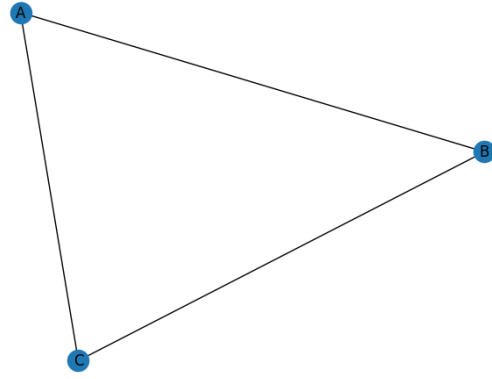


Figure 3: Undirected Graph

Which object the graph, nodes, and relationship between the nodes represent, depends on the state or system a graph tries to model. Moreover, edges in a graph can store weights, or as Majeed and Rauf, 2020 refer to as valued or non-valued representations of the strength between two nodes. While the visual representation of graphs offers intuitive appeal, having a more quantifiable format for efficient computer processing is essential. As Singh and Sharma, 2012 explain, graphs are best expressed through matrices.

A possible representation of a graph is those of an adjacency matrix. As defined by Singh and Sharma, 2012 an adjacency matrix A represents which nodes are adjacent to which other nodes. For N nodes present in a finite graph G , the adjacency matrix is $A = N * N$, where each entry $a_{ij} = \{1, \text{if there is an edge}, 0 \text{ otherwise}\}$. The diagonal, therefore, always represents the potential edge pointing back to the node itself, a self-loop. Based on this circumstance, it can be stated that the adjacency matrix will always be symmetric in the case of an undirected graph. Another critical metric in graph theory is the degree of a node. Kasiviswanathan et al., 2013 define the degree of a node $deg_n(G)$ for node $n \in N$ as the count of connected nodes. This definition of a node degree is in the case of an undirected graph. In the case of a directed graph, the degree is separated into the in-degree, the count of incoming nodes, and the out-degree, the count of outgoing nodes for a node $n \in N$. In the case of an undirected graph, the degree can easily be stored in a degree matrix $D = N * N$, which is filled with zeros except for the diagonal, indicating the count of connected nodes. In a directed graph, there exist two degree matrices, one for in- and another for the out-degrees of nodes. An example adjacency matrix and degree matrix, referring to Figure 3, are shown in Table 1, and Table 2.

Table 1: Adjacency Matrix

	A	B	C
A	0	1	1
B	1	0	1
C	1	1	0

Table 2: Degree Matrix

	A	B	C
A	2	0	0
B	0	2	0
C	0	0	2

The flexibility of graphs as a modelling tool enabled researchers to use graphs to model actual objects, entities, or systems. For example, Girvan and Newman, 2002 used graphs to model social networks, Kleinberg, 1999 modelled the World Wide Web, Newman, 2003 showed the usage of graphs in biology, including protein-protein interactions, and Hagmann et al., 2008 for modelling the human brain connectivity. While the papers mentioned above only show a glimpse of graphs' applicability to model objects or systems, they prove the general applicability and representative power of graphs.

Whereas the flexibility of graphs is immense, the irregularity of their structure can be challenging when trying to use them as input data for learning in graph domains. As explained by Battaglia et al., 2018, an explicit representation and an appropriate form of processing are needed to use a learning algorithm for computing interactions between entities and their relations. Since graphs are used to represent document images, they represent semi-structured data. As Šimsa et al., 2023 explain, this is due to their strong visual structure but varying layout. Despite being considered semi-structured, graphs as an input source are irregular data structures. They are considered irregular, as they may

have a variable size of unordered nodes and the number of neighbours is not fixed. Wu et al., 2020 explain that essential operations, such as convolutions, cannot simply be extended from an image to a graph domain. This circumstance led to the development of GNN and their successors, explained in the following chapter.

2.3 Graph Neural Networks

Gori et al., 2005, proposed the first graph neural network architecture in their paper 'A New Model for Learning in Graph Domains'. The authors propose a neural network architecture that enables the usage of graphs as direct inputs to machine learning by extending the prevalent usage of Recurrent Neural Network (RNN) from that time. The issue lies in the structure of graphs. Since graphs can have an arbitrarily large size and relations, the order in which nodes and their representations should be fed into the RNN was unclear. Using a form of graph traversal, such as Breadth-First Search (BFS) or Depth First Search (DFS) to determine an input order makes the output dependent on the initial node order. However, as shown in the study by Vinyals et al., 2015, the order in which sequences are fed into a Long-Short Term Memory Network (LSTM), are very decisive for the final performance.

Instead of converting a graph to an input sequence, GNNs use the graph as a whole as an input structure. Given a graph G and nodes N , each node stores information in a vector $x_n \in \mathbb{R}^s$ referred to as a *state*. However, since nodes can be connected via an edge to neighbouring nodes, x_n is naturally defined by the neighbourhood of n . To update the vector x_n , each vector is passed through a *transition function* f_w that incorporates the neighbouring states of each node. The transition function is a neural network with its own weights and biases. Iteratively, the states of each node are updated based on their state and those of their neighbours. Once the state at point x_{i+1} has a small difference from the state at time x_i , it is concluded that it has reached a *stable state*. The user must determine the exact difference for reaching a *stable state*. The weights learned from the neural network, thus, greatly impact when a *stable state* is reached. While the paper by Gori et al., 2005 proposes the first GNN architecture, Scarselli et al., 2008 provide a more detailed description of its architecture. While the two papers by Gori et al., 2005 and Scarselli et al., 2008 are milestones in developing GNNs, their implementations suffer some drawbacks. As Kipf and Welling, 2016 explain, iteratively updating node states in the hope that a stable state will eventually be reached is problematic since there is no guarantee that this will come into effect. In addition, the training and model architecture is complex,

challenging to implement in practice, and computationally expensive.

In difference to the neural network architecture proposed by Gori et al., 2005, Kipf and Welling, 2016 simplify the process of passing messages between the nodes by introducing the concept of convolutions from Convolutional Neural Networks (CNNs), effectively creating a GCN. The reasoning for this approach is simple. Traditional convolutions, for example applied to an image, slide over parts of the image with a filter to learn local hierarchies. Since graphs do not necessarily follow a grid-like structure, a different approach is needed to capture the local surrounding of a node. The layer-wise propagation rule of nodes to implement the behavior described above, can be denoted as:

$$H^{l+1} = \sigma(\tilde{D}^{-\frac{1}{2}} \tilde{A} \tilde{D}^{-\frac{1}{2}} H^{(l)} W^{(l)}) \quad (1)$$

The propagation rule can be broken down into steps that explain the base message-passing algorithm in a GCN. For N nodes in a graph, each node is described through d node features. A feature can effectively be any information that describes the node and is essential to a node's informative value. Node features can thus be represented as a feature matrix $X = N * d$. As explained by Kipf and Welling, 2016, self-connections are added to the adjacency matrix A by adding the identity matrix I : $\tilde{A} = A + I_n$, effectively filling the diagonal matrix with ones. Following this step, \tilde{A} is normalized by multiplying the modified adjacency matrix with the degree matrix D . As explained above, the degree of a node is the number of edges connecting to other nodes, stored as D_{ij} , with the diagonal indicating the degree of each node. The degree is normalized by taking the inverse square root to prevent higher-degree nodes from dominating the influence on the node features. To preserve symmetry in the matrix and account for the degree of the node sending the message, the inverse degree matrix is multiplied twice, so that: $\tilde{A} = \tilde{D}^{-1/2} * \tilde{A} * \tilde{D}^{-1/2}$. To complete the layer-wise propagation rule, \tilde{A} is multiplied with the node feature matrix H and a trainable weight matrix W . By wrapping an activation function, such as Rectified linear Unit (RELU), around this part of the equation, a new node feature representation for each node is generated: $H^{l+1} = \sigma(\tilde{D}^{-\frac{1}{2}} \tilde{A} \tilde{D}^{-\frac{1}{2}} H^{(l)} W^{(l)})$.

In the implementation described above, a convolution operation is strictly performed over a 1-hop neighbourhood, meaning the direct neighbours of a node n_i for $n \in N$. This aspect of the locality around a node is similar to that of a CNN for image classification. As shown by Wu et al., 2020 a filter applied to a patch of pixel values of an image is essentially a form of capturing the local neighbourhood around the centre node. Similarly, the implementation by Kipf and Welling, 2016

is a form of spatial-based graph convolution, as the representation of a node $n \in N$ is updated with the local neighbourhood information from nodes around the centre node n_i . Spatial methods have a straightforward translation from convolutions on images to the graph domain and have been implemented in various papers, such as Veličković et al., 2017, Monti et al., 2017, Gao et al., 2018, and many more. In contrast to spatial methods, spectral methods are based on graph signal processing. Spectral methods represent graphs using the graph Laplacian matrix, as shown by Wu et al., 2020 and Defferrard et al., 2016:

$$L = I - D^{-\frac{1}{2}} * A * D^{-\frac{1}{2}} \quad (2)$$

Here, I_n represents the identity matrix, $D^{-\frac{1}{2}}$, the normalised inverse degree matrix, and A , the adjacency matrix of graph G , assuming an undirected graph. In this case, L always contains real numbers and is symmetric, allowing for further graph-related operations. Assuming a graph signal x_i , which is a feature vector holding information about the graph nodes, a Graph Fourier Transform (GFT) can be applied. Similarly to audio signal processing, in which the Fourier transform decomposes an incoming signal into sine waves, the GFT decomposes the graph signal into eigenvectors of the Laplacian L . As shown by Wu et al., 2020, the inverse of the GFT is an exact representation of the incoming signals within the frequency domain, allowing for easier convolutions. A filter, analogous to a convolutional kernel in a CNN, is applied to the spectral representations after the Fourier Transform. The function helps to extract local features, similar to a filter of a CNN, before inverting the GFT and converting the representation back to the spatial domain. As Wu et al., 2020 explain and evident by the implication of the filter, the choice of filter is a significant driver for the expressiveness of the extracted structures.

An important GCN that uses a spectral method is the paper introduced by Defferrard et al., 2016. Its advantage lies in the definition of the filter applied. The filter is strictly localized and can control how far, in terms of nodes from the centre node, the filter expands. To do so, Defferrard et al., 2016 derive \tilde{L} , which is a transformation of the above-described Graph Laplacian, such that:

$$\tilde{L} = 2 * \frac{L}{\gamma_{max}} - I \quad (3)$$

Here γ_{max} denotes the largest eigenvalue of L and I , the identity matrix. Then, using Chebyshev polynomials, the filter size can be controlled via the parameter K . The Chebyshev polynomials can

formally be denoted as:

$$T_k(\tilde{L}) = 2 * \tilde{L} * T_{k-1}(\tilde{L}) \quad (4)$$

In this case $T_0(\tilde{L}) = I$ and $T_1(\tilde{L}) = \tilde{L}$. Finally, by applying a filter $g(\theta)$, a new representation is learned by a simple multiplication:

$$g(\theta) = \sum_{k=0}^{K-1} \theta_k * T_k(\tilde{L}) \quad (5)$$

θ represents parameters learned during training, similar to weights in a neural network. As visible, K expands the filter convolution by reaching k -hops nodes away from the centre node. The paper of Kipf and Welling, 2016 offer a simplified propagation rule than the one proposed by Defferrard et al., 2016. Nonetheless, both are widely-used implementations of convolutional operations on graphs, while one is spatial- and the other a spectral-based method.

While the convolutional operations on graphs, as described above, are still used today, they have some drawbacks concerning the nature of transductive learning. The node embeddings and weight matrix learned in the paper of Kipf and Welling, 2016 depend on the presence of all nodes within the graph. As a result, applying the learned weights to a scenario where some nodes are not present during training becomes nontrivial. Because the prediction for a node depends on the information from other nodes, the model may encounter difficulties during the absence of some nodes. This makes trained GCNs less applicable to handle graphs with new nodes added after training.

As Hamilton et al., 2017 explain, this is a big drawback in domains where input graphs evolve frequently, and unseen nodes might be encountered during testing. To alleviate this problem, the authors propose Graph Sample and AggregatE, GraphSAGE, a model capable of inductive learning. Instead of learning a weight matrix, node features are leveraged to learn an embedding function that can be applied to new nodes and unseen graph structures. As explained in the paper, three main steps are performed inside GRaphSAGE. At first, a fixed-size set of neighbourhoods is sampled around each node in the graph, reducing the computational footprint within a batch. Next, an aggregator function is wrapped around the features of the neighbourhood. Which aggregation function to use might depend on the task. As specified by Hamilton et al., 2017, a mean aggregation, LSTM aggregation, or pooling approach could be applied in this scenario, whereas the authors decided to use a max-pooling. Finally, the aggregated neighborhood is concatenated with the node's features and fed

through a fully-connected layer to generate a new embedding. The learned function is transferable between nodes as the weights are shared across nodes. A common denominator in each of the papers above is the fact that the neighbourhood of a node is incorporated into the node features, either by a convolution operation, Kipf and Welling, 2016, Defferrard et al., 2016 or by learning an embedding function, Hamilton et al., 2017. Inspired by the advancements of neural machine translation, Veličković et al., 2017 propose to extend the ability to deal with variable-sized inputs to the domain of graphs. By being able to focus on the most relevant parts of an input, the concept of self-attention is introduced, enabling the model to compute the representation of a single sequence. The idea is to learn a hidden state for each node based on its neighbours and a self-attention mechanism. As the operation is computationally efficient and also offers inductive learning, as in the paper of Hamilton et al., 2017, it offers a promising architecture called Graph Attention Networks (GATs). At first, the node features are fed through a linear transformation. Following this step, the attention scores are calculated, measuring the importance of a node to another. Across each node neighbourhood, the attention scores are normalized using a softmax function to attain a representation ranging between 0-1. The normalized attention scores are then used to compute a weighted feature matrix of each node's neighbours based on the attention scores. After being passed through a RELU activation function, the output features are obtained. The model learns independent attention-weighted functions and representations by employing multi-headed attention, meaning several different attention mechanisms and weights. The final representations are then concatenated and form the final embeddings.

While each model architecture explained above learns node embeddings or embedding functions differently, each method can be applied to similar downstream tasks. The three most prominent prediction tasks are node classification, edge classification (or link prediction), and graph classification, Wu et al., 2020. While each paper mentioned above implements some form of node prediction, only Gori et al., 2005, Scarselli et al., 2008, and Defferrard et al., 2016 implemented graph classification. The task of link prediction will be introduced in the later Chapter 4.1.5.2.

The flexibility of graphs as an input structure to represent relationships and entities enables a variety of use cases based on Graph Neural Networks. The paper by Kipf and Welling, 2016 first applied GCNs to a citation network to identify similar classes in a network, which can be seen as a form of social network analysis. Veličković et al., 2017, and Chen et al., 2020 used the same datasets, whereas

the latter also extended the usage to other social network datasets, such as YouTube, Flickr, and Blog-Catalog. Kearnes et al., 2016 applied GCNs to predict the molecular fingerprints based on molecular structure, whereas Veličković et al., 2017 tested their GAT model on protein-protein interaction. Apart from molecular chemistry, Ying et al., 2018 trained a GCN to generate node embeddings based on 3 billion pins and boards from Pinterest to build a high-quality recommendation engine, outperforming the current deep-learning architectures. Y. Li et al., 2017 use a graph model for traffic forecasting, while Yao et al., 2019 demonstrate the ability of GCNs for text classification.

In the scope of this paper, GCNs will be used for DU. There have been numerous attempts by Riba et al., 2019, Qasim et al., 2019, Holeček et al., 2019, Chi et al., 2019 and Lohani et al., 2019 to use graph-based models for different document-related tasks. Workist, the partner company of this paper and provider of the data exemplifies the usage of GCNs in practice to process complex documents, such as invoices, purchase orders, delivery orders, and many more.

2.4 Graph Neural Networks in Document Understanding

There have been few attempts to use GNNs or GCNs to understand documents, each with a slightly different focus. As explained before, valuable data is presented inside a table in many industries. Recognizing a table and extracting its content presents a valuable task to prevent the manual processing of documents. To challenge this task, Riba et al., 2019 represent documents as a graph with nodes capturing blocks of text and edges as spatial relationships between them. By training a GNN, they can classify whether a node is part of a table. Similar to this approach, Holeček et al., 2019 focus on tables and their content. However, by extracting features from input images and feeding through a pipeline of CNN and LSTM networks, they can extract the table's relationship between rows and columns. Qasim et al., 2019 take a similar approach and treat document pages as graphs, with text lines as blocks and edges representing spatial relationships. By doing so, they can classify nodes into categories and infer hierarchical relationships between them. Chi et al., 2019, dive deeper into recognizing complicated table structures like nested cells spanning multiple rows. They can extract information from the documents and recognize the internal table structure by proposing a two-step process of detecting cells via a Recurrent Convolutional Neural Network (R-CNN) and the recognition based on a graph-based method. In contrast, Lohani et al., 2019 focus less on identifying tables and their content but on extracting key-value pairs from inside the document to extract complex pat-

terns inside the document. While each paper has a different focus and uses different data, they present a valuable basis for understanding challenges and opportunities in graph-based representations to understand documents.

The common ground for each of the methodologies described above is that each uses some form of graph-based representation to understand the layout or content of the document. Lohani et al., 2019, Riba et al., 2019, Holeček et al., 2019, Chi et al., 2019, and Qasim et al., 2019, each use a method to infer edges based on spatial relations between the nodes. Edges are an essential aspect for capturing tabular structures in the document since, as Riba et al., 2019 point out, they offer a complementary dimension to the raw textual data. Riba et al., 2019, Lohani et al., 2019, Holeček et al., 2019, Qasim et al., 2019 all create nodes based on individual words, whereas Chi et al., 2019 create nodes based on cells, which could potentially contain multiple words separated by a white-space. While each of the paper state they are utilizing some form of spatial relationships to infer edges between each token, only Lohani et al., 2019 and Chi et al., 2019 point out their method for doing so. To reduce the number of edges to a reasonable size, Chi et al., 2019 infer edges between each token based on K nearest neighbor (KNN) method. In difference to this approach, Lohani et al., 2019 use a graph modelling algorithm that attributes words as part of horizontal lines, then reads words line by line and derives edges based on the vertical projection. While this approach is the best documented and reconstructable, it also poses some further advantages, as discussed in Chapter 4.1.2.1. In conclusion, no matter which method is chosen, creating relations in the graph based on the spatial relations of the document is a widely used method.

While each method transforms its documents into some graph-like representation, the networks trained are very different. Qasim et al., 2019 and Riba et al., 2019 use a GNN to classify nodes into different categories or as part of the table, respectively. While not explained in detail, Chi et al., 2019 use a graph-based method that is similar to that of a GNN. In contrast, Lohani et al., 2019 make use of a GCN, in detail the variant utilising Chebyshev polynomials as described in Chapter 2.3. Finally, Holeček et al., 2019 utilize a pipeline consisting of a CNN and LSTM to model the relationships between rows and columns. Since each method used is very different and part of a multi-step pipeline, it seems logical that the chosen network for learning the graph representation needs to be carefully evaluated depending on the use case.

The dataset used for training needs to be carefully evaluated to understand the implications of the results. Riba et al., 2019 utilize the CON-ANONYM and the RVL-CDIP dataset, containing of 960 and 518 images, respectively. Both datasets come from industrial and administrative sources, hand-labelled by the authors and scanned by ABBYY OCR. In comparison, Lohani et al., 2019 use a private dataset with 3100 invoices provided by a private company, hand-annotated by the authors at the word level. Tesseract OCR was the chosen tool for text extraction. In comparison, Holeček et al., 2019 used a smaller and a bigger dataset containing 4848 and 35880 PDF pages. The documents are of various vendors and layouts and annotated by hand and an algorithm. The tool used for extracting text from inside bounding boxes was not disclosed. Similarly, Chi et al., 2019 also created their dataset, SciTSR, for the task, containing 15000 tables in PDF format. The tables are created based on LaTeX source files, which are interpreted to infer the position of tables and text inside the document. Lastly, Qasim et al., 2019 also generated tables and content based on HTML source files to create a large dataset consisting of 500000 tables in total. Summarising the datasets used in each of the papers, the applicability of each result is hardly transferable between them since they are trained on specific documents and types. While some papers, such as Riba et al., 2019 use a small dataset, limiting the general expressiveness of their model to unseen data, Chi et al., 2019 and Riba et al., 2019 automatically generate the datasets based on source files. While the automatic creation of training data overcomes the issue of a small dataset, it creates the issue that the model will be biased to the specific input document type and not be transferable to a production scenario in which administrative documents are created from all sorts of sources. Artificial datasets are a vital restriction when analysing each paper's applicability since understanding structured layouts becomes much easier if the source of creation always follows the same rules and layouts. In the case of Chi et al., 2019, it is possible that the trained model performs much better on LaTeX source files, while it struggles with unseen document sources, such as Word, Excel, or documents coming from ERP systems.

Whereas the data sources are very different, many of the critical problems pointed out in the paper are similar. As Chi et al., 2019 point out, the structure of a table can become very complex, and many existing methods cannot cope with this complexity to extract reasonable results - an issue also encountered in this thesis. This problem is repeated by Holeček et al., 2019, stating that invoices usually suffer from very specialized structures. Moreover, document formats vary significantly in

their tabular layout, as pointed out by Riba et al., 2019. Therefore, Lohani et al., 2019 emphasise the need for a robust model to adapt to new structures for proper extraction. In addition, each of the papers, not automatically created from source files, needed to be hand-annotated - a significant constraint for creating models that can generalise on larger data volumes. However, even if larger datasets are created automatically from source files, the resulting images suffer from noise, such as different fonts and sizes, and in the case of administrative documents or scans, even physical damage, such as scratches or smudges.

While each paper plays a vital role in improving the task of DU and extraction, they also highlight the state and complexity of the current state of research. While some papers have achieved promising results, the trained model is hardly generalisable to data from unseen sources, emphasizing the need for more extensive and encompassing datasets, as well as novel and robust methods enough to capture the nuances and complexity of administrative documents.

3 Theoretical Frameworks

This section highlights fundamental concepts discovered in prior research that were adopted to the specific problem. At first, the task of identifying subgraphs is introduced, after which an essential pre-processing step called node labelling is explained. Finally, the specific problem of line item detection is discussed based on prior research.

3.1 Subgraph Learning via Graph Convolutional Neural Networks

There have been very few attempts to explicitly learn subgraph representations, partly based on the difficulty of representing subgraphs. A subgraph must be formally defined to clarify these circumstances. Based on the definition by Wang and Zhang, 2022, let $G = (N, E, X)$ be a graph described through a finite node set N , a set of edges E , and a node feature matrix X , whose i^{th} row describes the feature of node i . A subgraph $S = (N_s, E_s, X_s)$ is a subgraph of G if $N_s \subseteq N$ and $E_s \subseteq (N_s * N_s) \cap E$ and X_s is a stack of rows that correspond to the nodes within the subgraph. In essence, this definition points out that every node in the subgraph S must also be part of the larger graph G , as every edge in the subgraph S must also be part of the larger graph G . Since each node is described through a row in the feature matrix, the rows corresponding to the nodes that are part of S correspond to the feature matrix X_s . Applying this definition to the use-case of this thesis, it becomes evident that each

line item that is part of a document graph qualifies as a subgraph in the larger document graph G . While this could be expected, predicting subgraph structures reveals several challenges. Alsentzer et al., 2020 point out four main issues in the scope of subgraph learning:

1. **Varying Structure and Size:** Subgraphs are not necessarily a repeatable pattern that is easily identified within the main graph. Instead, they can be spread out, vary in size, and be placed far apart. Alternating sizes and structures also occur in line items since they do not necessarily encompass a single line but several ones, with alternating amounts of tokens. The question is how to represent these subgraphs effectively.
2. **Internal and External Connectivity:** Subgraphs are seldom isolated structures but connect to nodes outside the subgraph. Since message passing inside a GNN is performed based on the edges, external connectivity will also influence subgraph representation - raising the question of how to account for external connections.
3. **Location inside the larger Graph:** Subgraphs could be situated anywhere inside the larger graph - either concentrated in one area or spaced apart. Learning the correct position and the effect on predicting subgraphs is crucial.
4. **Shared edges and nodes:** Subgraphs likely share the same edges or non-edges, making subgraphs dependent on each other. Since the data in the scope of this thesis is reduced to line item tokens only, subgraphs are always connected, increasing the difficulty of distinguishing them.

In their paper, Alsentzer et al., 2020 presented the first novel approach to tackle the task of subgraph learning - SUBGNN. The training is initialised by setting an anchor patch, A_i , a set of nodes from the corresponding subgraph S_i that is adjacent to but not inside the subgraph. Following this step, each node has features assigned to them. The main innovation then lies in a three-channel message passing that deals with the issues mentioned above of subgraph learning. The first channel corresponds to internal messages that capture the subgraph and its structure. Incoming messages, the second channel, are computed based on messages passed from the anchor patch into nodes inside the subgraph. Finally, outgoing messages, the third channel, capture messages passed from inside the subgraph to nodes in the anchor patch. Each channel is separately aggregated and then concatenated before passing it through a neural network layer to update the node features based on a learnable weight matrix. While this proves to help learn subgraph representations, it is not fit for the problem at hand since

it does not perform the task of subgraph detection but subgraph representational learning. Subgraph representational learning is similar to the task of graph prediction, in which representations of whole graphs are computed, just with the modification that the representation refers to a subgraph within a larger graph.

However, a few aspects, as pointed out by Wang and Zhang, 2022 make using SUBGNN complex in practice. At first, the three-channel message passing proposed is computationally expensive and challenging to implement. Moreover, the proposed approach depends on the initial definition of anchor patches. In a task such as line item prediction, where the position and number of line items are unknown prior, the implementation becomes difficult in practice. Instead, Wang and Zhang, 2022 propose a different operation, a node labelling propagation step instead of the three-channel message passing. The usage of such node labels has been proposed in various papers, such as Wang and Zhang, 2022, Zhang et al., 2021, Zhang and Chen, 2018, P. Li et al., 2020 and You et al., 2021.

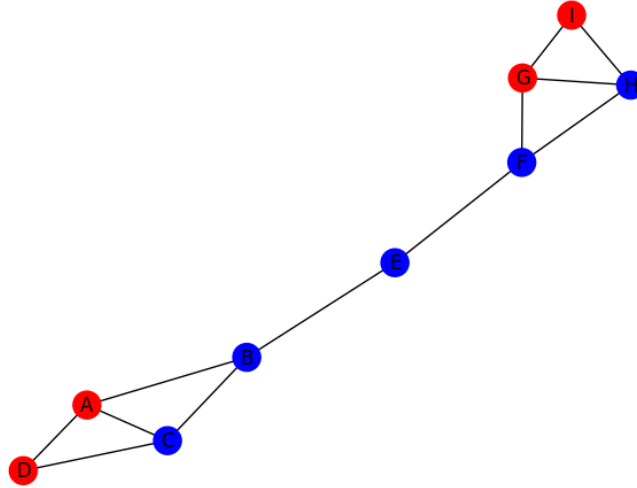
The theoretical implications and different implementations of Node Labelling are discussed in the following chapter. The node labelling method used by Wang and Zhang, 2022 implies an easier-to-implement and more accurate subgraph representation. The label propagation layer starts with assigning a label to each node based on its position or the relation within the subgraph. Following this step, one message passing round is performed, collecting and aggregating information from the neighbour. Finally, an activation function is wrapped around the updated feature vector to ensure the values stay within a suitable range. Afterwards, the message passing of choice is performed, while further label propagation steps could be deployed later in the model. This modified architecture, GNN with Labelling Tricks for Subgraph Representation Learning (GLASS), outperforms most of the baselines and performances of SUBGNN.

3.2 Node Labelling

The concept of labelling nodes has been used in various studies and has proven useful when used correctly in the scope of the problem. An example from Zhang et al., 2021 is introduced to motivate the usage of node labelling. Assuming a graph as in Figure 4, nodes (I, G) and (A, D) are isomorphic. Graph isomorphism, as defined by McKay et al., 1981 occurs for two graphs, G_1 and G_2 , if a one-to-one mapping exists that enables to map the nodes of G_1 onto G_2 , such that the adjacency of two

nodes in G_1 are adjacent to those of G_2 . In easier words, graph isomorphism occurs when every node in the first graph has a counterpart in the second graph and vice versa. A node-pair in the first graph connected by an edge must always have an exact counter-pair in the second graph. While the example shown in Figure 4, does not have two graphs, it does, however, have two perfectly isomorphic sub-graphs such that without the labels, it would be impossible to distinguish between the node pair (I, G) and (A, D) . As Zhang et al., 2021 conclude, this creates difficulties in many graph-related tasks, such as link prediction. When performing several hops to incorporate neighbouring attributes and update the node features, nodes I and D would have the exact representation due to the similarity of the neighbourhood. For example, predicting which node is more likely to link with (F) would become difficult in this scenario. The abstract example proposed can be directly transferred to the problem of line item classification since many line items are repetitive and isomorphic by nature. Therefore, distinguishing a node in line item x from a node in line item $x - 1$ might become challenging when the local neighbourhoods are indistinguishable. To mitigate this issue, node labelling forces each node to have unique characteristics that enable the graph to distinguish one node from the other.

Figure 4: Isomorph Graph



A more straightforward node labelling method, proposed by Zhang et al., 2021 involves applying a one-hot label for nodes that are part of a subgraph S . By doing so, representations are learned at a subgraph instead of a node-level, which performs better than Alsentzer et al., 2020. Depending on the prediction task, the node labelling is adjusted accordingly. Zhang et al., 2021 propose a labelling

method that assigns the same label to the two target nodes in a link prediction case and iteratively assigns larger nodes the further they are from the two centre nodes. This way, the structural information of the enclosing subgraph is incorporated into the nodes. In comparison, P. Li et al., 2020 incorporate the distance between nodes to create unique node features. The distance is calculated based on a set of reference nodes. The distance could be based on a shortest path or a diffusion-based method. In either scenario, the node feature will provide additional context based on the relationship to other nodes. You et al., 2021 instead uses node colouring to encode unique identities to distinguish the nodes from each other. While node labels are either assigned based on attributes information, such as Zhang et al., 2021 or position P. Li et al., 2020, You et al., 2021 focus on assigning unique identities to each node. Incorporating a one-hot vector into the node features distinguishes the nodes from each other. This approach is quite different as the one-hot label carries no semantic information. Since node labelling proved a successful method to overcome graph isomorphism, it is adopted in the scope of this thesis and added as a node feature. The exact details are explained in Chapter 4.1.3.11.

3.3 Line Item Detection

Lastly, some more papers need to be addressed to narrow in on line item prediction. While there have been many advancements in document analysis via OD algorithms, Schreiber et al., 2017, Šimsa et al., 2023, or Smock et al., 2022, the task of analysing documents based on graph methods is relatively sparse. In particular, line item detection is rarely the sole focus of papers based on GNNs or GCNs. The only two papers implicitly dealing with line item detection are: "Table understanding in structured documents", by Holeček et al., 2019, and "Complicated Table Structure Recognition", by Chi et al., 2019. While the focus of both papers has been explained in Chapter 2.4, the line item detection task has not been explicitly investigated. Holeček et al., 2019 use the whole document as input and try to classify nodes. One of these categories is line items, which are represented inside a table in the document. While training the model on a smaller dataset and achieving a promising result of an F1 score of 93%, it is unclear whether the aspect of line item detection tried to identify separated line items and their enumeration as labels or to label all tokens as line items inside the table body. Nonetheless, the result seems promising and shows that the task of line item detection is possible. On the other hand, Chi et al., 2019 focused on more complex table structures. The evaluation of models on complex tables achieved a Micro F1 score of 72,5%, which is decent but highlights the issue of

detecting line items spanning several lines in a table. In this thesis's scope, line items usually span multiple lines and do not necessarily follow a regular grid-like structure. Therefore, Chi et al., 2019 results seem more relevant to the proposed problem. However, the data used by Chi et al., 2019 is based on LaTeX-source files making it easier for a model to understand formatted tables than tables created by different ERP systems, as in the case of this study.

4 Methodology

The methodology highlights the decisions made for modelling, their reasons and expected outcomes. The data will be introduced at first, including all necessary pre-processing steps and the different target labels used during training. Following this explanation are the modelling methodology, training, and evaluation methods.

4.1 Data

This section explains the provided data and pre-processing steps taken. At first, the data is analyzed and described to capture the complexity and nuances of it. Following the introduction, the creation of edges, nodes, and edge features and the different prediction tasks are explained.

4.1.1 Description

The data used in this study consists of Customer Order Documents used for processing orders between B2B transactions of Small-to-Medium-sized Enterprises (SMEs) across many European markets and the United States. Due to different document sources, languages can vary between English, French, Spanish, German, and many others. Moreover, the documents are created based on different ERP systems and are not standardised based on a single source. The pages inside a document might also be copied and skewed and include noise from smudges, tilting, or poor resolution. Each document is split into individual pages, and treated as a single instance, meaning one page equals one graph as an input to the model.

The data provider is Workist, a company that challenges DU. Founded in 2019, the company operates in B2B transactions by extracting relevant information from business documents into a machine-readable format. By doing so, Workist offers a seamless information exchange between various parties, such as customers, distributors, and clients.

Since the data is processed along a pipeline inside a DU service of Workist, the training documents

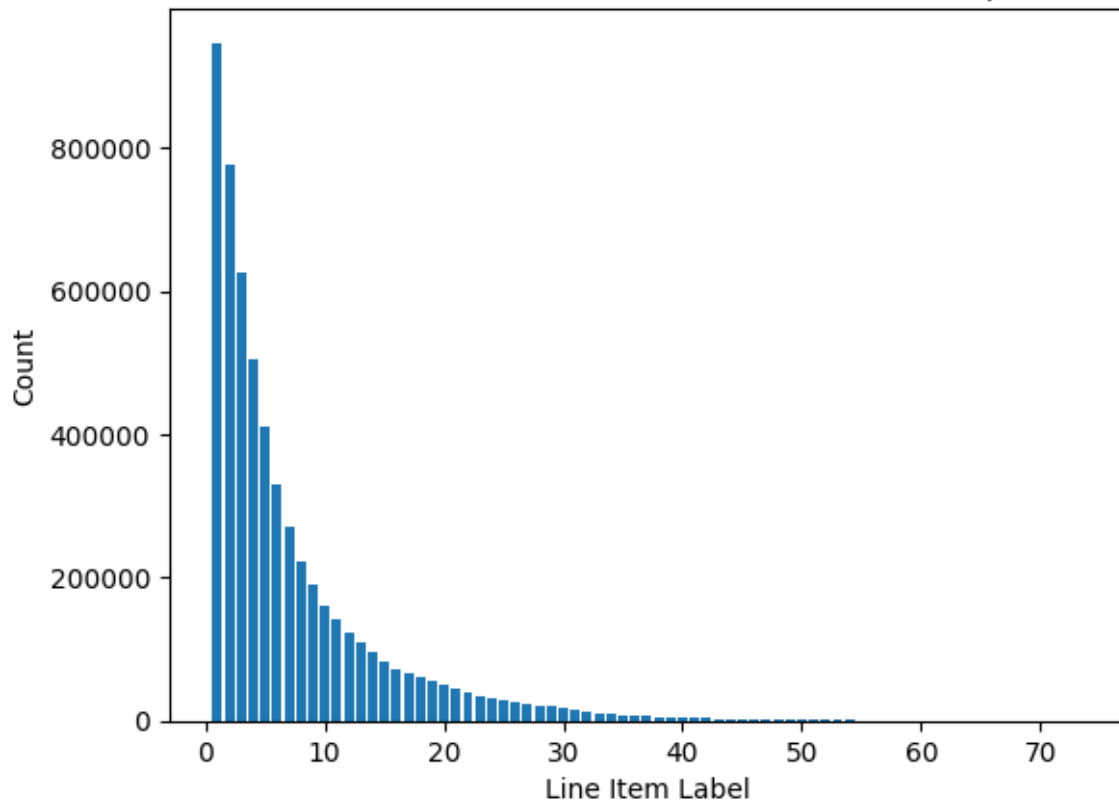
already contain valuable information before modelling. At first, each document is analyzed via OCR, which detects tokens and their position in the document. A token is any character, letter, or digit containing informative content; a white space separates that. The concept of tokens is essential since one coherent text might be separated into several tokens. For example, the text *steel bolts* would be separated into the tokens *steel* and *bolts*. Furthermore, the OCR tool identifies the position as a bounding box coordinate $bbox = [coord_{left}, coord_{top}, coord_{right}, coord_{bottom}]$ relative to the page's width and height. Moreover, it converts the character into a string containing the content.

Following the OCR step, the tokens are transformed into a graph $G = (N, E)$, where N is a set of tokens identified prior by the OCR and E edges between the tokens that are created based upon a methodology by Lohani et al., 2019, explained in the following chapter. The resulting graph is used as an input to a GCN that classifies each node into a category, which explains its function within the document. In total, there exist over 70 different categories. Example categories are *OrderLineItemSupplierArticleNumber*, *OrderLineItemDescription*, *OrderLineItemCurrency*, and more. Finally, each page is converted into an image and used as input into an OD model that identifies essential areas on the page. These are, for example, a table, a header, and individual line items. The classified tokens can now be assigned to each line item based on the overlap of the bounding box. The last part is to be replaced by a GCN.

4.1.2 Data Pre-processing

Each document is converted into a graph with tokens as nodes to enable the learning of graph representations of documents. For each node, the available information is stored as node features. The same amount of features are available for every node and stored in a matrix $X = N * d$, with N being the number of nodes and d the number of features. Each document is different in its layout and not limited in the number of line items. Since the line item amounts are not fixed, they result in imbalanced line item counts within the dataset, as visible Figure 5.

Figure 5: Distribution of line item tokens



Tokens not part of a line item are excluded to reduce noisy tokens in the graph. As a result, each input document is transformed from an empty graph Figure 6, to a document graph with all tokens, Figure 7, and finally to a document with only line item tokens, Figure 8. This pre-processing step simplifies the training for the model, as it reduces the random noise around the relevant line item tokens by eradicating all tokens that are not part of it. This step is feasible in a production scenario since the token classification model should already identify the relevant line items. Indeed, the model performance would be impacted by any earlier miss-classification of the token classification model. However, this is an acceptable risk outside of identifying line items. Consequently, this step immediately drops all documents without line items since training and testing are unnecessary. In addition, all documents containing only a single line item are dropped. Even though this step might seem irrational and suffers from a form of data snooping, as this information would not be available to the model beforehand, it will be argued in Chapter 7 that this information can be confidently inferred beforehand.

Brasius GmbH | Hemminger Weg 34-36 | D-47433 Klee
 Winkler GmbH
 c/o BRB vordruck
 Holstenlandstraße 6-8
 D-10119 Berlin

Bestellung

Bestell-Nr.: 1234567890
 Datum: 08.08.2020
 Sachbearbeiter: 123 Meier, Stefan

Tel.: 01234-1234
 Fax: 01234-1235

Seite: 1

Artikel	Menge	Einheit	Preis	Gesamt ELR
Lieferanschrift: Firma Brasius GmbH Hemminger Weg 36 47533 Klee				
Geschäftstyp: Lager				
Lieferdatum: 12.08.2020				
Pos. 1: 00012345 Eckwinkel, abgerundet, gelb-vz 120x120x20 mm Verpackungseinheit VE	20,000	40 STCK	0,41	16,40
Pos. 2: 00012346 Schnurband, gelb-vz 400x20x15 mm, CP 12,50x4 Verpackungseinheit VE	10,000	30 STCK	1,75	52,50
Pos. 3: 00012347 Schnurband, gelb-vz, weibl. 80x120x40 mm Verpackungseinheit VE	20,000	40 STCK	1,14	45,60
Pos. 4: 00012348 Tuchband, gelb-vz 75x75x15 mm				
Übertrag				114,50

Figure 6: Empty Graph

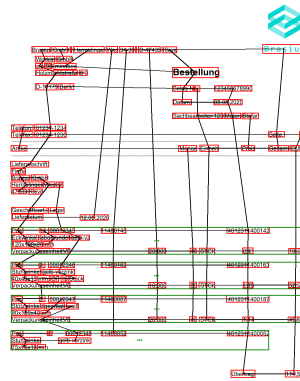


Figure 7: All Tokens

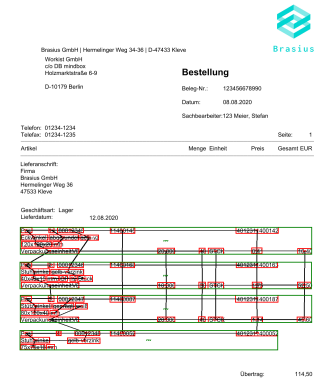
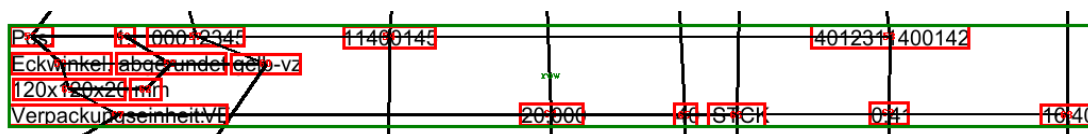


Figure 8: Only Line Item Tokens

4.1.2.1 Edge Creation

As explained, nodes within the graph are the tokens detected by the OCR tool and labelled as part of a class. The question of how to connect the nodes within each graph plays a central role as it directly influences the message-passing algorithm of the trained model. The idea of generating edges is based on the proposed implementation by Lohani et al., 2019. In the paper, the authors describe an algorithm to infer a grid-like representation of edges between the tokens by connecting each token to the closest neighbouring tokens in a horizontal and vertical dimension. This approach offers numerous improvements compared to a brute-force approach that would connect each token to all available tokens in the document. At first, the resulting graphs are more computationally efficient, as they significantly reduce the number of edges. Secondly, it limits the degree of each node to four edges, and it infers some form of ordering since nodes can be understood in a horizontal or vertical ordering. This ordering mirrors the arrangement of words in the document and the writing in natural language, as shown in Figure 9, traversing from left to right, starting at token *Eckwinkel*, would correctly result in the text *Eckwinkel abgerundet gelb-vz*.

Figure 9: Single Line Item



4.1.3 Node Features

Node features used as an informative source for training are based on the content of the token. Since the node features represent individual tokens and are frequently updated through neighbouring nodes, they play a vital part in the model's ability to learn how to represent nodes within the graph. A single feature vector for a node is based on several data sources. Each feature is explained through its calculation below.

4.1.3.1 Normalised Bounding Box Coordinates

Since each token stored within a node is fenced through a bounding box rectangle, each node has bounding box coordinates available as spatial features. The bounding box coordinates are stored based on their top, left, right and bottom coordinates. Since non-normalised features can cause deep learning models to suffer from vanishing and exploding gradients during backpropagation, bounding box coordinates are normalised based on a document page's width and height:

$$Coords_{\text{norm}} = \left(\frac{coord_{\text{top}}}{height}, \frac{coord_{\text{left}}}{width}, \frac{coord_{\text{right}}}{width}, \frac{coord_{\text{bottom}}}{height} \right) \quad (6)$$

4.1.3.2 Relative Position

The bounding box coordinates are compared to the table coordinates to capture the relative position of each token's bounding box within a page. Therefore, the bounding box centroids are calculated for the X and Y coordinates:

$$X_{\text{centroid}} = \frac{X_{\text{left}} + X_{\text{right}}}{2} \quad (7)$$

$$Y_{\text{centroid}} = \frac{Y_{\text{top}} + Y_{\text{bottom}}}{2} \quad (8)$$

The table width and height are merely the difference between the right/left and bottom/top coordinates, respectively:

$$Table_{\text{width}} = X_{\text{right}} - X_{\text{left}} \quad (9)$$

$$Table_{\text{height}} = Y_{\text{bottom}} - Y_{\text{height}} \quad (10)$$

The relative X and Y coordinates for a node are calculated as follows:

$$X_{\text{relative}} = \frac{X_{\text{centroid}} - Table_{\text{left}}}{Table_{\text{width}}} \quad (11)$$

$$Y_{\text{relative}} = \frac{Y_{\text{centroid}} - Table_{\text{top}}}{Table_{\text{height}}} \quad (12)$$

By doing so, each node receives relative X and Y coordinates within the relative space of the table area.

4.1.3.3 Word Indices

Since the word indices are enumerated integers based on the token classification model, they must be normalized to prevent exploding gradients during model training. Word indices are normalized using the min and max index, like the bounding box coordinates. For each word index, the following transformation is applied:

$$Index_{normalised} = \frac{Index - Min_{index}}{Max_{index} - Min_{index}} \quad (13)$$

4.1.3.4 Label Encodings

Since the nodes were classified prior by a token classification model, each node had a label assigned to it. Overall, there are over 60 labels present. Example labels are *OrderCustomerNumber*, *OrderInvoiceAdressEmail*, *OrderProjectNumber*. Node features are processed into node labels using scikit-learn's LabelEncoder, and the resulting integer labels are one-hot encoded using scikit-learn's OneHot Encoder. Finally, each label was represented by a 72-dimensional vector.

4.1.3.5 Betweenness

The betweenness centrality of a node is a graph metric that captures the node's centrality within the graph. In mathematical terms, it is the sum of the fraction of all shortest paths for a node pair (s, t) that pass through the node v . If N is the set of nodes of a graph G , then the betweenness centrality of node v is denoted as:

$$B(v) = \sum_{s, t \in N} \frac{\sigma(s, t|v)}{\sigma(s, t)} \quad (14)$$

, where s and t are all other nodes in the network.

4.1.3.6 Edge

Edge is a one-hot encoded feature vector, indicating whether a neighbour exists in that direction for the possible four coordinates (left, top, right, bottom). In mathematical terms, $edge = (e_{left}, e_{top}, e_{right}, e_{bottom})$ is a four-dimensional vector, where for each direction i :

$$e_i = \begin{cases} 1, & \text{if edge exists.} \\ 0, & \text{otherwise.} \end{cases} \quad (15)$$

4.1.3.7 Distances

Similarly to the above vector, distances is a feature vector indicating the distance calculated by the edge creation method of Lohani et al., 2019. Therefore, the equation is adopted to be $distance = (d_{left}, d_{top}, d_{right}, d_{bottom})$ so that for each direction i :

$$d_i = \begin{cases} distance_{edge}, & \text{if edge exists.} \\ 0, & \text{otherwise.} \end{cases} \quad (16)$$

4.1.3.8 Horizontal Edge

Each token can have two horizontal edges (e_{left}, e_{right}) , whereas the token to the left or right could be of the same token class as the source node. The node feature Horizontal Edge, is, therefore, a two-dimensional vector (e_{left}, e_{right}) where for each direction i :

$$e_i = \begin{cases} 1, & \text{if target node is of same token class.} \\ 0, & \text{otherwise.} \end{cases} \quad (17)$$

4.1.3.9 Vertical Edge

Analogous to the above feature, each token can have two vertical edges (e_{top}, e_{bottom}) . The node feature Vertical Edge is, therefore, a two-dimensional vector (e_{top}, e_{bottom}) where for each direction i :

$$e_i = \begin{cases} 1, & \text{if target node is of same token class.} \\ 0, & \text{otherwise.} \end{cases} \quad (18)$$

4.1.3.10 Degree

The final feature, the degree of the node, is a one-dimensional vector. As explained in Chapter 2.2, the degree in an undirected graph represents the number of edges for a node i . Based on the edge creation method chosen, each node can, at max, have four edges in the coordinates, summing up the edges gives the total amount of edges, $sum_{edge} = sum(e_{left}, e_{top}, e_{right}, e_{bottom})$, where for each edge:

$$e_i = \begin{cases} 1, & \text{if edge exists.} \\ 0, & \text{otherwise.} \end{cases} \quad (19)$$

4.1.3.11 Node Colouring

As explained in Chapter 3.2, labelling nodes as information in the node features before training the model can boost the performance. Due to the issue of graph isomorphism and the non-trivial enumeration of line items from a node perspective, a node labelling trick was used to boost the learning. The node labelling in this thesis is based on node colouring, which associates nodes with colour, indicating the potential line item. While it is challenging to assign such colours for many nodes, after all, the problem of line item detection is the use case, it is feasible to identify candidate nodes as root nodes within each line item. Since each document is based on a Latin language, read from left to right and top to bottom, line items consequently originate on the left side. In addition, line items follow repeatable patterns - though not necessarily alike from the content, the columns in a table ensure consistency among the vertical domain. Based on these aspects, axioms about the creation of tables are defined:

1. **Table Root Node:** Within each document graph, $G = (N, E)$, with N being a set of nodes and E a set of edges, a list of top-left tuples $C = (top, left)_1, (top, left)_2, \dots, (top, left)_3$ can be created, storing the top-left-coordinates for each node in the graph. When calculating the min of this list, $L_{min} = \min(C)$, the tuple minimising the function can be extracted. Since line items are always enumerated from 0 to i for i line items present and read from left to right and top to bottom, the smallest top-left tuple, indicating the node on the top left, must always be part of the first line item. This node is called a root node.
2. **Parallelism:** Since line items, even in the case of spanning cells in the horizontal and vertical direction, always follow a grid-like representation, line items in a table must always run parallel.
3. **Horizontal Connectivity:** Parallelism implies that any pair of tokens (n_1, n_2) that are part of N and align horizontally must always be part of the same line item. If this were not the case line items could cross each other and not follow a grid-like structure.
4. **Root Node Connectivity:** Besides a horizontal grid-like structure, tables have a vertical structure. For each document graph G , the nodes of one line item form a subgraph S_i , with i being the line item number, so that $S_i \subseteq G$. Due to the abovementioned condition, an existing subgraph S_{i+1} must be placed below for any subgraph S_i . Otherwise, line item two could come after three, not following a logical enumeration. This enumeration implies that for each node

$n_i \in S_{i+1}$, the top-left tuples of all nodes in S_{i+1} must be below the top-left tuples of all nodes in S_i . Therefore, when traversing the graph vertically, starting from the root node in S_1 , all other subgraphs in G will eventually be encountered.

5. **Root Node Classes:** Concluding the axiom of Root Node Connectivity, it is crucial to consider the labels L assigned to each node in N . Since each node has a label assigned to it, given by the token classification model and indicating the function inside the table, a final axiom can be stated. The successful identification of the root node n_1 and its label l_1 , determine the root for the first subgraph S_1 in G . Since each subgraph S_i describes a line item that is placed in a grid-like structure, each line item must contain a node $n_i \neq n_1$ which has the same token label. Since the labels are arranged based on their function in a columnar layout, the additional root nodes with the same token label must be encountered when traversing the graph vertically and indicate the next root node of a subgraph $S_i \neq S_1$.

Furthermore, the axioms lay the groundwork for a node feature encapsulating global line item structures on a node level. A recursive algorithm was developed based on the axioms, which performs the node colouring and is described in the pseudo-code below:

Algorithm 1 Node Colouring

Require: A graph $G = (N, E, X)$, with N being a set of nodes and E a set of edges. X is a feature matrix $X = d * N$, with d being the amount of features, including the bounding box coordinates of a token. Each node is initiated with an empty colour and can point to max 4 neighbours.

- 1: Initialise empty root node, root node list and empty root token class
 - 2: **for** each node in N **do**
 - 3: Store the node bounding box top and left values
 - 4: **end for**
 - 5: Minimise over the sum of stored bounding box values to update root node and class
 - 6: Append root node to root node list
 - 7: Initiate list of candidate root nodes
 - 8: Call **Algorithm 2: Explore-candidates-recursively** using bottom neighbour of root node
 - 9: **for** each node in candidate root nodes **do**
 - 10: Call **Algorithm 3: Determine-most-left-node** with left neighbour of candidate root node
 - 11: **end for**
 - 12: **for** updated left nodes in candidate root nodes **do**
 - 13: **if** left node label is equal to root token class and has a right neighbour **then**
 - 14: Append most left node to root node list
 - 15: Assign new node colour to root node
 - 16: **end if**
 - 17: **end for**
 - 18: **for** each root node in root node list **do**
 - 19: Call **Algorithm 4: Horizontal-recursive-run** with right neighbour of root node and node colour of root node
 - 20: **end for**
-

Algorithm 2 Explore-candidates-recursively

Require: Bottom node b

- 1: **if** $b \neq \text{None}$ **then**
 - 2: Assign b to list of candidate root nodes
 - 3: Call **Algorithm 2: Explore-candidates-recursively** using bottom neighbour of b
 - 4: **end if**
-

Algorithm 3 Determine-most-left-node

Require: Left node l

- 1: **if** $l \neq \text{None}$ **then**
 - 2: Call **Algorithm 3: Determine-most-left-node** with left neighbour of l
 - 3: **else**
 - 4: **return** l
 - 5: **end if**
-


Algorithm 4 Horizontal-recursive-run

Require: Right node r and node colour c

- 1: **if** $r \neq \text{None}$ **then**
 - 2: Assign node colour c to node r
 - 3: Call **Algorithm 4: Horizontal-recursive-run** with right neighbour of r
 - 4: **end if**
-

The algorithm performs four main steps. At first, it determines the root node by minimising the top-left tuples of each node. Then it traverses the graph vertically by exploring all the root node's bottom neighbours. Each neighbour with the same token class as the root node is deemed a root node for another line item. By traversing horizontally to the right neighbours of each root node, all neighbours that are part of the same line item are found. Figure 10 visually shows the implementation of these axioms, with the red square indicating the initial root node, orange squares the candidate root nodes and blue squares the tokens encountered during horizontal recursion.

Figure 10: Node Colouring approach



Brasius GmbH | Hermelinger Weg 34-36 | D-47433 Kleve

Workist GmbH
c/o DB mindbox
Holzmarktstraße 6-9
D-10179 Berlin

Bestellung

Beleg-Nr.: 123456678990
Datum: 08.08.2020
Sachbearbeiter: 123 Meier, Stefan

Telefon: 01234-1234
Telefax: 01234-1235

Seite: 1

Artikel	Menge	Einheit	Preis	Gesamt EUR
Lieferanschrift: Firma Brasius GmbH Hermelinger Weg 36 47533 Kleve				
Geschäftsart: Lager Lieferdatum: 12.08.2020				
Pos. 1: 00012345 11400145 4012311400142				
Eckwinkel, abgerundet gelb-vz 120x120x20 mm Verpackungseinheit/VE	20,000	40 STCK	0,41	16,40
Pos. 2: 00012346 11400163 4012311400163				
Stuhlwinkel gelb-verzinkt 40x40x15 mm, GP 12 Stück Verpackungseinheit/VE	10,000	30 STCK	1,75	52,50
Pos. 3: 00012347 11400087 4012311400187				
Stützwinkel, geprägt, weiß 80x120x40 mm Verpackungseinheit/VE	20,000	40 STCK	1,14	45,60
Pos. 4: 00012348 11400052 4012311400052				
Stuhlwinkel gelb-verzinkt 75x75x16 mm				
		Übertrag:		114,50

Red rectangle indicates root node

Orange rectangles indicates candidate root nodes

Blue rectangles indicates horizontal connectivity

4.1.4 Edge Features

Since the tokens are connected via edges, the distance between the bounding box of two connected tokens can be computed and added as a distance attribute to each edge. The distances are used as the basis for determining an edge feature:

4.1.4.1 Normalised Inverse Distances

Distances between bounding boxes are normalised as a basis for edge weights. At first, for a given document graph $G = (N, E)$, with N being a set of nodes and E a set of edges and d_i denoting the distance for edge i , the inverse distance of each edge $e \in E$ was calculated by:

$$d_{inv_i} = \begin{cases} \frac{1.0}{d_i}, & \text{if } d_i \neq 0. \\ 0, & \text{otherwise.} \end{cases} \quad (20)$$

Next maximum and minimum inverse distances are found:

$$id_{max} = \max(d_{inv_1}, d_{inv_2}, \dots, d_{inv_i}) \quad (21)$$

$$id_{min} = \min(d_{inv_1}, d_{inv_2}, \dots, d_{inv_i}) \quad (22)$$

Finally, the normalised, inverse distances nid_i are calculated:

$$nid_i = \frac{id_i - id_{min}}{id_{max} - id_{min} + \epsilon} \quad (23)$$

, in which ϵ denotes a tiny constant to prevent division of zero error. The computation is essentially a form of min-max-normalisation to ensure that the distances within each document graph can only range between $(0, 1)$.

Within the context of the GCNs, the normalised inverse distances are treated as edge weights during forward propagation. When aggregating features from neighbouring nodes, the features are multiplied by the weights of the edge connecting to that node. A higher weight consequently contributes more to the node features. Conversely, a lower weight contributes less.

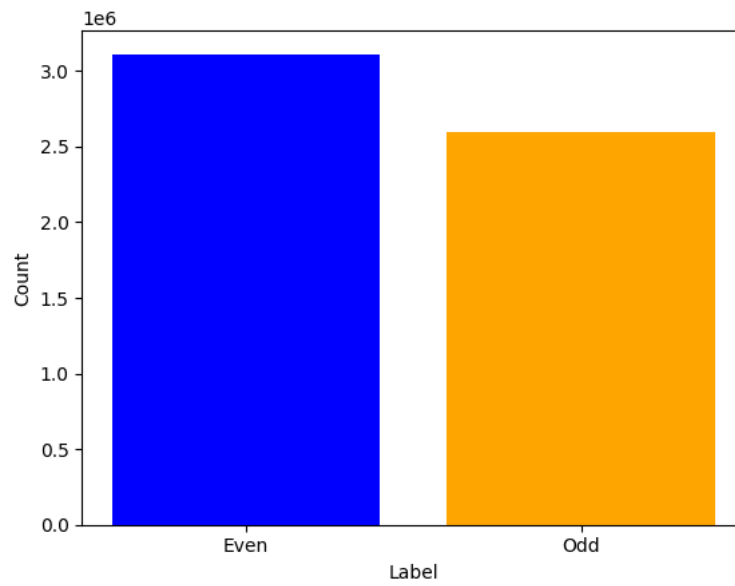
4.1.5 Target Labels and Training Tasks

The predicted labels are compared against different true labels to calculate the loss of the model after each iteration and update the weights. Different true labels mean that different targets and approaches are used to model the task of inferring line item structures:

4.1.5.1 Binary Even-Odd Prediction

The first node prediction task used binary labels as true labels for each node. Even though the number of line items per document varied and consequently the number of line item classes, each node can be classified as being on an even or an odd line item. When counting the line items available from top to bottom, each node can be classified as belonging to either one of the two. Per each document, each node had a binary label assigned to it, making it a binary classification task. Even though this approach does not directly predict the line item number, it has interesting properties to make it a more feasible prediction task. At first, assigning binary labels to the nodes will solve the issue of an imbalanced dataset. As explained in Chapter 4.1.2, the amount of line items per page is imbalanced across all pages. The ratio of even and odd nodes is more balanced when using binary labels, as shown in Figure 11. Additionally, there is a more nuanced reason why binary labels are preferable over enumerated ones. The task is a node prediction task, and passing messages in the graph between nodes creates weights and node embeddings used to infer a label. As graphs do not naturally have a direction, it is unclear from the node point-of-view which node should have a higher label than another. Since line items have similar structures, including the same arrangement, token classes, and content, inferring an order from this information is counterintuitive without a direction. Especially for many line items on a page, assigning a large numerical value, such as 60, and a smaller one, for example, 2, based on comparable node embeddings, is a difficult task even for a human. While this problem is not solved in the binary classification case, it is mitigated since the logic of alternating zeros and ones are simpler than enumerated numbers.

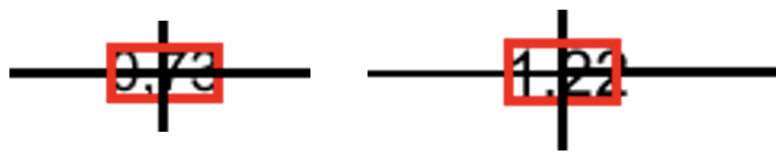
Figure 11: Distribution of even-odd labels



4.1.5.2 Link Prediction

A comparison is made with two example nodes, shown in Figure 12, to elaborate on the challenge described above.

Figure 12: Single Token comparison



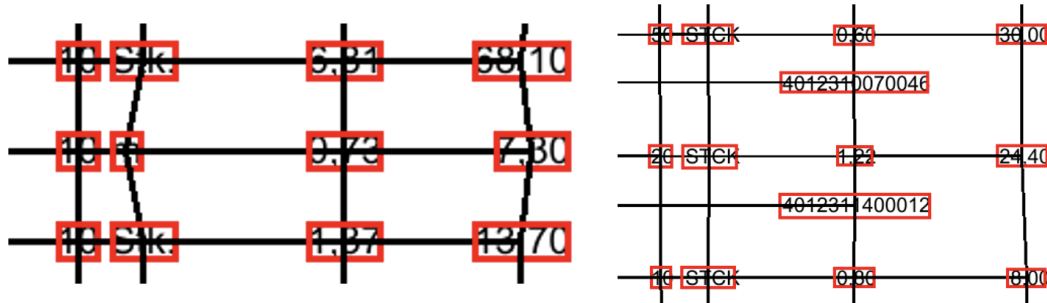
Token left: Text - 0.73, Token Class - *OrderLineItemUnitPrice*, Left - 0.7936, Top - 0.4404

Token right: Text - 1.22, Token Class - *OrderLineItemUnitPrice*, Left - 0.7266, Top - 0.4311

Each node is part of a line item with the same token class, *OrderLineItemUnitPrice*, and a similar position in the document. The task is to infer the line item number. This example shows that inferring a line item based on single node features is rarely better than random guessing, even for humans.

Even when presenting the local context around the node, as shown in Figure 13, it is challenging to guess the line item correctly.

Figure 13: Single Token comparison within neighborhood context



The actual line item number can be inferred only when presented with the overall graph, shown in Figure 22 and Figure 23. This example highlights the difficulty of inferring an enumeration of line items. The task of inferring an enumeration is alleviated by predicting which edges correctly connect nodes on the same line item. The notion for this approach is based on the idea that after a few convolutional rounds, the network will eventually create meaningful node embeddings between nodes on the same line item. While it is still challenging to correctly attribute these node embeddings to an integer value, comparing pairs of nodes for their similarity of node embeddings becomes more realistic. Node similarity is calculated through the cosine similarity between each pair of nodes connected through an edge and compared against the true value. Similar node embeddings should achieve a score closer to 1, implying that the edge correctly connects a node-pair on the same line item, while a score closer to -1 implies an incorrect edge between a node-pair not on the same line item. While this task does not directly identify line items, it does help rule out incorrect edges in the hopes of creating disconnected subgraphs for each line item. The simplicity of this approach, paired with the interpretability, makes it a handy approach, as proven later during the evaluation of results.

4.1.5.3 Line Item Prediction

Finally, the last task available to train is the extension of the binary prediction of Chapter 4.1.5.1 by directly predicting the line item number. Effectively, the class imbalances described in Chapter 4.1.2 are accepted by necessity. While the issues with this approach have been pointed out in-depth in the previous two chapters, it is helpful to tackle this challenge nonetheless, at least for reasons of

comparability. Using this approach also implies that a biased assumption is made toward the number of line items. Since a fix-sized last layer is needed to predict line item classes, the total number of line items across all pages must be known prior. While this information can be extracted from the available data, it might not represent reality accurately since documents with higher line item counts are likely to exist in reality. The trained model, however, will always be limited to the fixed-size layer.

4.2 Modelling Methodology

The target labels described beforehand lay the groundwork for approaching the task through three different methods: even-odd line item prediction, link prediction, or line item prediction. Since each method approaches the task of predicting line items from a slightly different perspective, the training and evaluation also differ. Overall, the graph architecture chosen for learning the line item representations is the GCN based on Chebyshev spectral graph convolutions proposed by Defferrard et al., 2016. The reason for the choice is motivated by the paper Lohani et al., 2019, since the edge creation method of this paper was adopted, and it achieved promising results in a comparable node classification task in documents. Additionally, spectral methods can capture more information about the surrounding local neighbourhood for predicting subgraph structures on a node level than a spatial method.

For each training task, a separate model was trained in Python 3.9.15. The model architectures are based on the PyTorch library 1.12.1, with the models loaded from torch-geometric 2.2.0. A Nvidia Tesla M60 8GB GPU was used for training.

4.2.1 Training Methodology

The three targets are trained separately on the same data before evaluating the resulting models on an unseen test set. Optimal parameters are determined based on hyperparameter tuning used for the models in the final evaluation. The data used for training was processed such that each document available for training contained at least two line items. The motivation and implications for this step were explained in Chapter 4.1.2 and will be discussed again in Chapter 7. Each model's weights are initialised based on the Xavier/Glorot Initialisation explained in Glorot and Bengio, 2010. Neural network weights and biases are randomly initialised. However, choosing randomisation and its scale is crucial since it can lead to exploding or vanishing gradients during backpropagation. Therefore, Glorot and Bengio, 2010 propose a weight initialisation based on a normal distribution around the

centre 0, which effectively creates random weights that are more symmetric, preventing the issues above during backpropagation. The optimiser chosen for the three tasks is Adam, with a weight decay set for the learning rate. The choice of Adam is motivated in part by comparable papers dealing with the task of document understanding, such as Lohani et al., 2019 and Holeček et al., 2019. The weight decay is a form of regularisation that adds a penalty term to the loss function, motivated by Krogh and Hertz, 1991, such that the modified loss L' is calculated by:

$$L' = L + \frac{1}{2}\lambda\|\mathbf{w}\|^2 \quad (24)$$

Here λ denotes the penalty term, and $\|\mathbf{w}\|^2$ is the squared L2 norm of the weight vector. The exact choice of learning rate and weight decay is explained in Chapter 5. A step learning rate scheduler was implemented with a step size of 20 and a gamma of 0.1. After 20 epochs, the learning rate is multiplied by gamma, forcing the learning rate to decay over time.

The loss function for the two node classification tasks (even-odd line items, enumerated line items) is the negative log-likelihood loss. For the link-prediction case, binary cross-entropy with logits loss was chosen. The negative log-likelihood loss is a standard loss function for multi-classification tasks and well-suited for the multi-classification task when predicting all line item numbers. Since each node in the graph exclusively belongs to one label, negative log-likelihood is preferable as it predicts out-labels separately for each token. Due to this condition, the loss function was also adopted for the even-odd prediction task. Regarding the link-prediction task, the input values for the loss function are slightly different from the node classification task. As explained, the results of the cosine-similarity scores between a node pair in the graph cause the resulting scores to range between -1 and 1 . Within the binary cross entropy with logits loss, the values are first passed through a sigmoid activation function, mapping them to values between 0 and 1 . The resulting values are well-suited for applying a cross-entropy loss to measure the difference between predicted and true labels. A dropout ratio was chosen after each convolutional layer in the model architecture to prevent the model from overfitting. Dropout is a very effective yet simple measure to prevent overfitting and was proposed by Srivastava et al., 2014. By randomly picking a certain amount of output nodes that are ignored for predictions, the model becomes less sensitive to specific weights. The choice of a , the ratio of picked nodes, is a measure for controlling the number of nodes dropped. The parameter a was tuned, and the optimal value is explained in the following chapter. Gradient Clipping is an additional measure to prevent

exploding gradients, first introduced by Pascanu et al., 2013. Gradients are scaled back to a threshold to prevent them from becoming overly large. In the scope of this thesis, the chosen threshold was set to 0.5. The overall training time and computational overhead are reduced as the model is constantly evaluated on the validation set during training. None of the data contained in the training is part of the validation set. The validation set serves two purposes. At first, it enables performance tracking on unseen data, while training is the basis for an early stopping mechanism. The mechanism stores the best performance of the model on the validation set at epoch i , and updates it in case there is an improvement. The training is aborted if no improvement occurs after x epochs since the model does not improve. In training, early stopping was set to a size of 20.

4.2.2 Tuning Methodology

Within the training, there is a multitude of parameters to be tuned to optimise the model performance. While it is not feasible to train all parameters in combination, a subset of relevant parameters was selected for tuning. The list of parameters are: Batch Size, Dropout Ratio, Hidden Neurons, Learning Rate, Weight Decay, Amount of Convolutional Layers, K (for Chebyshev Convolutional Layer). The exact values to be chosen for each parameter are shown in Table 3.

Table 3: Parameter ranges of tuning

K	BS¹	Layers	Dropout	HN²	LR³	WD⁴
2	16	2	0.3	256	$1e^{-4}$	0.01
3	32	3	0.5	512	$1e^{-5}$	0.001
4	64	4	0.7	1024	$1e^{-6}$	

¹ Batch Size;

² Hidden Neurons;

³ Learning Rate;

⁴ Weight Decay

A random search was chosen for tuning, as it has been proven more effective than a grid search, Bergstra and Bengio, 2012. Since training runs on the complete data are time-consuming, the number

of searches was limited to 25 and performed twice, once for the link-prediction task and once for the even-odd prediction task. As the prediction task and loss function is the same, the results of the even-odd prediction task are also chosen for the direct line-item prediction task. The exact results of each tuning run, including the optimal parameters, are shown in the following chapter.

Plenty of other relevant tuning parameters were neglected during tuning. However, this thesis focused on showing how to model the task. The same random state was set for each tuning run, creating the same train-test splits. The overall tuning time took roughly 240 hours.

4.2.3 Evaluation Methodology

The best-performing parameters identified by the tuning are used for the final models to test the performance. Each final model was trained three times with a separate random state, and the results were averaged to minimise the effect of a sampling bias. Each model was tested on unseen test data created from the same random state to prevent data leakage. Accuracy, Micro and Macro F1, Precision, and Recall are calculated to evaluate the model performance. The Precision, Recall, and F1 score are also reported for the individual prediction classes of each task to enable a deeper understanding of the direction of errors in the model.

The accuracy in a classification case is the proportion of correctly classified nodes/edges over the whole amount of nodes/edges predicted during training or testing:

$$\text{Accuracy} = \frac{\text{Number of correct predictions}}{\text{Total number of predictions}} \quad (25)$$

While it is a useful standard metric, it does not generate enough insights and can be misleading in the case of imbalanced data sets. The F1 score is based on Precision and Recall. The calculation of Precision is shown below, and is defined based on Buckland and Gey, 1994 as the number of retrieved relevant items over the number of retrieved items. By doing so it shows the ability to correctly identify relevant items. In the case of the even-odd predictions, a positive prediction implies an even line item and a correct edge in the link-prediction scenario.

$$\text{Precision}(P) = \frac{\text{True Positives}(TP)}{\text{True Positives}(TP) + \text{False Positives}(FP)} \quad (26)$$

The Recall, as defined by Buckland and Gey, 1994, is the number of retrieved relevant items or true positives out of all relevant items. Therefore, it implies how well a model is able to identify relevant

instances.

$$\text{Recall}(R) = \frac{\text{True Positives}(TP)}{\text{True Positives}(TP) + \text{False Negatives}(FN)} \quad (27)$$

The F1 score is then the harmonic mean between the two, balancing the result of each inside a single number:

$$F1 = 2 * \frac{\text{Precision} * \text{Recall}}{\text{Precision} + \text{Recall}} \quad (28)$$

In difference to the above calculation, the Micro F1 score calculates the total true positives, false negatives, and false positives for each class and therefore captures a potential class imbalance:

$$\text{Micro F1} = 2 * \frac{\sum_i TP_i}{\sum_i TP_i + 0.5 * (\sum_i FP_i + \sum_i FN_i)} \quad (29)$$

The Macro F1 score calculates the results for each class separately and then averages the results, meaning it does not account for class imbalance:

$$\text{Macro F1} = \frac{1}{n} \sum_{i=1}^n F1_i \quad (30)$$

In the scope of the data used, both metrics are useful. Micro F1 is essential, especially for the case of directly predicting line items, as it accounts for class imbalances, while the Macro F1 is helpful as each line item is equally important, independent of the class balance in the data.

5 Artefact Description

This chapter focuses on describing the artefacts generated within this study's scope. In total, three different types of models were trained, tuned, and tested that are available for further usage. The first model was trained for a node classification task by assigning binary labels to each node. The second model was trained to predict whether each edge in a graph correctly connects a node pair on the same line item. Lastly, another node classification model was trained to assign specific class labels for each line item. Each model was based the architecture of Chebyshev spectral graph convolutions, by Defferrard et al., 2016.

5.1 Model 1: Even-Odd Prediction

The first artefact created is a trained, tuned, and tested model designed to predict a binary label (0, 1) for each node in the graph. A zero indicates an even, and a one an odd line item. Based on the pre-processing of the data explained in Chapter 4.1.2, it is assumed that each input graph only contains line

item tokens. As explained above, the architecture used for training the model was based on Defferrard et al., 2016, as it has proven to work successfully in a related document understanding task by Lohani et al., 2019. Additionally, since the edge creation method by Lohani et al., 2019 was adopted for each input graph, the resulting graphs had a similar edge frequency for each node. The best-performing parameters for the binary classification case are documented in Table 12, displayed in the appendix. Moreover, the parallel coordinate chart provided in Figure 14 indicates the most relevant parameters of the successful training runs, reinforced by the parameter importance concerning the F1 score in Figure 15. While this task does not explicitly predict line items, it will be argued later in Chapter 7, that it is feasible to infer the enumeration if even-odd labels are predicted.

Figure 14: Parallel Coordinates Plot, Even-odd Prediction

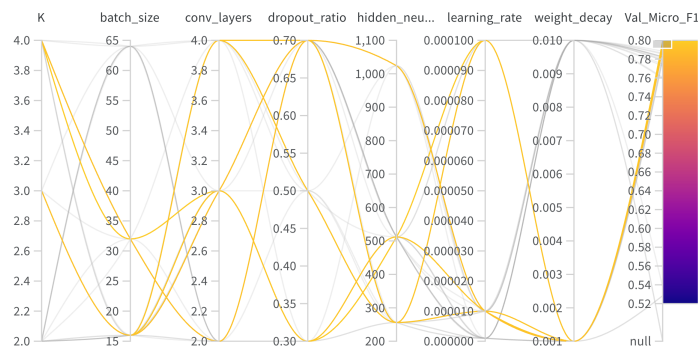


Figure 15: Parameter Importance, Even-odd Prediction

Config parameter	Importance ① ↓	Correlation
hidden_neurons	<div><div></div></div>	<div><div></div></div>
K	<div><div></div></div>	<div><div></div></div>
conv_layers	<div><div></div></div>	<div><div></div></div>
batch_size	<div><div></div></div>	<div><div></div></div>
learning_rate	<div><div></div></div>	<div><div></div></div>
dropout_ratio	<div><div></div></div>	<div><div></div></div>
weight_decay	<div><div></div></div>	<div><div></div></div>

5.2 Model 2: Link Prediction

The second artefact is another trained, tuned, and tested model designed to predict a binary label (0, 1) for each edge in the graph. A 0 indicates an incorrect edge, connecting a node pair of different

line items, while a 1 connects a node pair on the same line item. As evident by the tuning results in Table 13, this task performs much better than any of the other artefacts. Similarly, as before, the parallel coordinate chart in Figure 16 and the parameter importance in Figure 17, indicate the most relevant parameter for the model. While this task does not predict line items at all, it does modify the graph as a structure to isolate line item subgraphs. By deleting irrelevant edges and keeping relevant ones, the input graph is ideally pruned to S isolated subgraphs for S line items in the table. The results are discussed with different examples in Chapter 7.

Figure 16: Parallel Coordinates Plot, Link Prediction

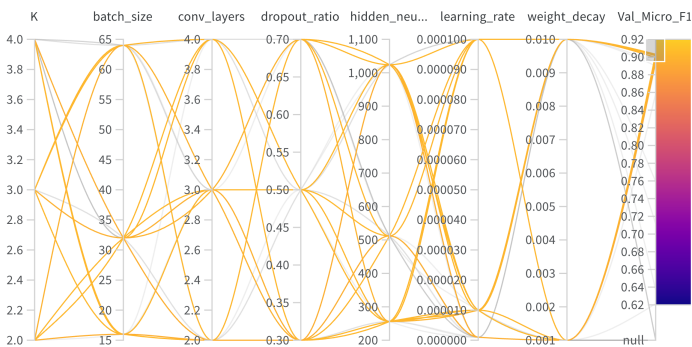


Figure 17: Parameter Importance, Link Prediction

Config parameter	Importance ① ↓	Correlation
learning_rate	<div><div></div></div>	<div><div></div></div>
conv_layers	<div><div></div></div>	<div><div></div></div>
dropout_ratio	<div><div></div></div>	<div><div></div></div>
weight_decay	<div><div></div></div>	<div><div></div></div>
K	<div><div></div></div>	<div><div></div></div>
hidden_neurons	<div><div></div></div>	<div><div></div></div>
batch_size	<div><div></div></div>	<div><div></div></div>

5.3 Model 3: Line Item Prediction

The last artefact created in this chapter is a trained and tested model designed to assign integer labels to each node, $1 - x$ for x line items in the graph. The model was not separately tuned, but the other node classification model parameters were adopted.

6 Evaluation of Results

6.1 Performance on unseen Data

Overall 44646 document graphs are used for training, testing, and evaluation. The documents are pre-processed, as explained in Chapter 4.1.2. 20% of the data is reserved for testing, meaning 8929 document graphs. The same amount of data is used for validating the model's performance during training. Therefore, each model was trained on 26788 documents in total. Each training task was evaluated three times with a different train-test-split to reduce a potential sampling bias. Therefore, the performance results presented are averaged across three training runs, with different random states for splitting the data. The standard deviation of each run is also reported to capture any deviations between the runs.

6.1.1 Model 1: Even-Odd Prediction

The performance of the first model, predicting even-odd line items, is presented in Table 4. The first row presents the model performance on all the data available. On average, the model has a 78% accuracy and Micro F1 score, with a slightly lower Macro F1 score. The Micro Precision and Recall score is the same since micro-averaging the results globally by summing the per-class true and false positive counts will result in the same values. Therefore, the accuracy is also equal to the Micro F1 score.

The data was split into buckets and evaluated separately to highlight better and worse-performing document cases. The rows represent the buckets, easy, medium, and hard graphs. An easy graph is considered a graph in which a line item does not extend a single line, creating a near-perfect grid, shown in Figure 24. A medium graph, presented in Figure 25, is a document graph in which line items span up to three lines, meaning up to three tokens vertically stacked. Finally, a hard graph is any document graph in which line items contain more than three lines in a single line item, as shown in Figure 26. Out of all 44646 documents with more than one line item, 20189 are considered easy, 8771 medium, and 15686 as hard graphs. The results for the even-odd prediction task indicate that the model performs much better for easier graphs. In contrast, the performance drops significantly from roughly 84% to 68% Macro F1 score. These results demonstrate that the model struggles with increasing complexities of data but also that the overall level of difficulty of document graphs in the

test set varies dramatically. The difference between the Macro Precision and Recall indicates that the model is slightly more likely to incur false negatives than false positives. Lastly, since documents with single line items were excluded in training, though they represent a realistic example encountered in an application scenario, they were added back in a separate test run. The test data results, including the single line items, are shown in the last row, "All difficulties incl. SLI". The results show that the performance does not decrease compared to the data excluding single line items in the first row. Instead, the performance is even slightly better. This circumstance can be explained by the fact that documents containing a single line item are easily marked via the node colouring method and, thus, instead, increase the amount of correctly labelled nodes.

The direction of error committed by the model can be understood when looking at Table 5. The results show the F1 score, Precision, and Recall, for the individual target labels, referring to an even or odd line item. The values are also averaged across three seeds. The results show that the model can predict both target labels decently. Overall, the model performs slightly better at predicting even line items, which does not come as a surprise, as there are generally more even line items present. Since there exists no real trade-off between performing better in one than the other class, it is difficult to say which case weighs more in those prediction scenarios.

Table 4: Performance, Even-odd Prediction

Data Used	Accuracy	Micro			Macro		
		F1	Precision	Recall	F1	Precision	Recall
All difficulties	0,7801	0,7801	0,7801	0,7801	0,7746	0,7983	0,7776
	$\pm 0,0162$	$\pm 0,0162$	$\pm 0,0162$	$\pm 0,0162$	$\pm 0,0255$	$\pm 0,0120$	$\pm 0,0242$
Easy graphs	0,8424	0,8424	0,8424	0,8424	0,8407	0,8515	0,8413
	$\pm 0,0034$	$\pm 0,0034$	$\pm 0,0034$	$\pm 0,0034$	$\pm 0,0062$	$\pm 0,0103$	$\pm 0,0078$
Medium graphs	0,7592	0,7592	0,7592	0,7592	0,7508	0,7824	0,7559
	$\pm 0,0233$	$\pm 0,0233$	$\pm 0,0233$	$\pm 0,0233$	$\pm 0,0378$	$\pm 0,0128$	$\pm 0,0341$
Hard graphs	0,7021	0,7021	0,7021	0,7021	0,6853	0,7300	0,6972
	$\pm 0,0389$	$\pm 0,0389$	$\pm 0,0389$	$\pm 0,0389$	$\pm 0,0679$	$\pm 0,0045$	$\pm 0,0527$

continued

Table 4: Performance, Even-odd Prediction

Data Used	Accuracy	Micro			Macro		
		F1	Precision	Recall	F1	Precision	Recall
All difficulties incl. SLI¹	0,7825	0,7825	0,7825	0,7825	0,7760	0,7991	0,7788
	$\pm 0,0137$	$\pm 0,0137$	$\pm 0,0137$	$\pm 0,0137$	$\pm 0,0247$	$\pm 0,0124$	$\pm 0,0265$

¹ Single Line Items

\pm indicates the standard deviation for averaged values across three seeds

All values are rounded to four decimal places

Table 5: Results per target, Even-odd Prediction

Target label	Precision	Recall	F1
Even line item	0,7889	0,8203	0,7964
	$\pm 0,0770$	$\pm 0,1215$	$\pm 0,0123$
Odd line item	0,8076	0,7348	0,7529
	$\pm 0,1009$	$\pm 0,1695$	$\pm 0,0623$

\pm indicates the standard deviation for averaged values across three seeds

All values are rounded to four decimal places

6.1.2 Model 2: Link Prediction

The performance of the link prediction task is shown in Table 6. Overall the performance is better than the even-odd prediction task. While the performance on all data is roughly around 90% accuracy and 89% Macro F1 score, the performance drops when switching from easy to hard graphs. The accuracy drops around 4% when going from easy to hard graphs, and the Macro F1 score is around 7%. The re-

sults also indicate that the model struggles with more complex documents. However, the performance is not impacted as much as the even-odd prediction case, suggesting that the model performance is overall more robust. In addition, the standard deviation for accuracy and F1 scores is much lower than the even-odd prediction task, indicating the model can easier reproduce the performance even with different train-test splits. When including single line items in the data, the performance stays the same.

The results concerning individual target labels indicate a solid performance for both targets, as shown in Table 7. The model correctly identifies correct edges around 95% of the time. In contrast, the model is more prone to misclassify incorrect edges, potentially leading to higher false positives. In the scope of the use case of identifying line items, this trade-off is acceptable. Since the task is to detect line items by creating connected subgraph structures, it is more critical to disconnect edges between tokens on the same line item than the other way around. While it would be ideal for balancing both cases, the cost of leaving some incorrect vertical edges between line items is an acceptable drawback.

Table 6: Performance, Link Prediction

Data Used	Accuracy	Micro			Macro		
		F1	Precision	Recall	F1	Precision	Recall
All difficulties	0,9001	0,9001	0,9001	0,9001	0,8863	0,9007	0,8759
	$\pm 0,0004$	$\pm 0,0004$	$\pm 0,0004$	$\pm 0,0004$	$\pm 0,0005$	$\pm 0,0006$	$\pm 0,0008$
Easy graphs	0,9227	0,9227	0,9227	0,9227	0,9193	0,9286	0,9135
	$\pm 0,0004$	$\pm 0,0004$	$\pm 0,0004$	$\pm 0,0004$	$\pm 0,0005$	$\pm 0,0002$	$\pm 0,0006$
Medium graphs	0,8842	0,8842	0,8842	0,8842	0,8636	0,8795	0,852
	$\pm 0,0004$	$\pm 0,0004$	$\pm 0,0004$	$\pm 0,0004$	$\pm 0,0005$	$\pm 0,0006$	$\pm 0,0008$
Hard graphs	0,8914	0,8914	0,8914	0,8914	0,8458	0,8569	0,8362
	$\pm 0,0007$	$\pm 0,0007$	$\pm 0,0007$	$\pm 0,0007$	$\pm 0,001$	$\pm 0,0012$	$\pm 0,0013$
All difficulties incl. SLI¹	0,9049	0,9049	0,9049	0,9049	0,8913	0,9042	0,8817
	$\pm 0,0017$	$\pm 0,0017$	$\pm 0,0017$	$\pm 0,0017$	$\pm 0,0021$	$\pm 0,0012$	$\pm 0,0026$

continued

Table 6: Performance, Link Prediction

Data Used	Accuracy	Micro			Macro		
		F1	Precision	Recall	F1	Precision	Recall

¹ Single Line Items

± indicates the standard deviation for averaged values across three seeds

All values are rounded to four decimal places

Table 7: Results per target, Link Prediction

Target label	Precision	Recall	F1
Incorrect Edge	0,9063	0,8064	0,8535
	±0,0019	±0,0092	±0,0060
Correct Edge	0,9022	0,9554	0,9280
	±0,0032	±0,0002	±0,0017

± indicates the standard deviation for averaged values across three seeds

All values are rounded to four decimal places

6.1.3 Model 3: Line Item Prediction

The results for predicting line item numbers are visible in Table 8. As evident, the performance is lower than the other two training tasks, which is to be expected given the difficulty of 73 imbalanced target labels. Interestingly, the performance is not much worse than the even-odd prediction task, with a Micro and Macro F1 score of 73%. Moreover, the drop in performance between Easy, Medium and Hard graphs are similar compared to the change for even-odd labels. Same as before, the model performs better, with a Micro F1 of 79% and Macro F1 of 80%, on easier graphs, compared to more

difficult ones, with 72% for Micro F1 and 65% Macro F1. The ratio between Macro Precision and Recall behaves contrary to the other two models. Especially for medium and hard graphs, the model likely misses many node instances where a line item is present. Reintroducing single line items causes a much better performance concerning the Macro F1 score averaged across three seeds. This behaviour is due to the model’s ability to detect line item one more accurately than higher-order line items. Since 73 target labels were available for prediction, the model was not evaluated for individual targets.

Since this model was trained for a multi-classification task with 73 targets but used the same data as the binary classification task, the performance is expectedly worse. Nonetheless, the model could learn from the data and achieve a competitive performance against the other node classification task.

Table 8: Performance, Line-item prediction

Data Used	Accuracy	Micro			Macro		
		F1	Precision	Recall	F1	Precision	Recall
All difficulties	0,7382	0,7382	0,7382	0,7382	0,7407	0,7336	0,7756
	$\pm 0,0074$	$\pm 0,0074$	$\pm 0,0074$	$\pm 0,0074$	$\pm 0,0537$	$\pm 0,0581$	$\pm 0,0357$
Easy graphs	0,7940	0,7940	0,7940	0,7940	0,8063	0,8101	0,8237
	$\pm 0,0062$	$\pm 0,0062$	$\pm 0,0062$	$\pm 0,0062$	$\pm 0,0452$	$\pm 0,0647$	$\pm 0,0219$
Medium graphs	0,7286	0,7286	0,7286	0,7286	0,6597	0,6468	0,7206
	$\pm 0,0033$	$\pm 0,0033$	$\pm 0,0033$	$\pm 0,0033$	$\pm 0,0604$	$\pm 0,0536$	$\pm 0,0786$
Hard graphs	0,6725	0,6725	0,6725	0,6725	0,4165	0,3731	0,5624
	$\pm 0,0091$	$\pm 0,0091$	$\pm 0,0091$	$\pm 0,0091$	$\pm 0,1229$	$\pm 0,1075$	$\pm 0,1552$
All difficulties incl. SLI¹	0,7349	0,7349	0,7349	0,7349	0,7755	0,7824	0,7908
	$\pm 0,0026$	$\pm 0,0026$	$\pm 0,0026$	$\pm 0,0026$	$\pm 0,0455$	$\pm 0,0450$	$\pm 0,0383$

¹ Single Line Items \pm indicates the standard deviation for averaged values across three seeds

All values are rounded to four decimal places

6.2 Ablation

The performance of the models is tested in an ablation study to show feature importance and potential interactions. One feature at a time is removed before training the model again on the available data and reporting the performance on a validation set. The complete list of features is *Label Encoding*, *Betweenness*, *Relative Position*, *Degree*, *Edge*, *Distances*, *Normalized Bboxes*, *Horizontal Edge*, *Vertical Edge*, *Node Colouring*. Features are removed from left to right, implying that the last run only contains *Node Colouring* as a feature.

As shown in Table 9, the training run, including all features, achieved the highest performance on the validation set. Nonetheless, the gap in performance between a single feature, *Node Colouring*, and all features is only about one per cent. While there is likely some impact from other features, this difference indicates that the most relevant learning is already contained in the first feature, *Node Colouring*.

Table 9: Ablation Study, Even-Odd Prediction

No. of Features	Accuracy	Micro F1	Macro F1
10	0,7941	0,7941	0,7941
9	0,7936	0,7936	0,7936
8	0,7931	0,7931	0,7931
7	0,7916	0,7916	0,7916
6	0,7917	0,7917	0,7917
5	0,7613	0,7613	0,7449
4	0,7613	0,7613	0,7449
3	0,7902	0,7902	0,7902
2	0,7901	0,7901	0,7900
1	0,7857	0,7857	0,7855

All performance values correspond to tests on a validation set

All values are rounded to four decimal places

The results of the ablation study of the link prediction task are shown in Table 10. The results indicate no significant differences between individual runs, and no interactions are visible after removing a feature, similar to the results before. Since the performance of the *Node Colouring* is similar to the run with all features, this feature alone is likely the most decisive for both model’s prediction.

Table 10: Ablation Study, Link Prediction

No. of Features	Accuracy		Micro F1	Macro F1
	Precision	Recall		
10		0,9019	0,9019	0,8895
9		0,8917	0,8917	0,8774
8		0,9011	0,9011	0,8884
7		0,9020	0,9020	0,8896
6		0,9014	0,9014	0,8890
5		0,9014	0,9014	0,8889
4		0,8998	0,8998	0,8864
3		0,8989	0,8989	0,8852
2		0,8983	0,8983	0,8847
1		0,8992	0,8992	0,8851

All performance values correspond to tests on a validation set

All values are rounded to four decimal places

7 Discussion and Limitations

Within the scope of this thesis, it has been shown that the task of learning node representations to infer line item association is feasible. While the best-performing task, link prediction, did not learn line items directly, predicting even-odd line items on a node level was also proven possible, yet less performant. Predicting line item numbers directly on a node level suffers from complications arising from the imbalance of line item numbers, the uncertainty regarding the maximum amount of line

items across all documents, and the difficulty of enumerating node labels.

Different post-processing steps must be discussed to address the results and show that the first two tasks could be used in a production environment. At first, when predicting the links between nodes, the ideal resulting graph should have x amount of isolated subgraphs for x amount of line items in the document graph. While the success of inferring links can alternate, as shown in Figure 27 and Figure 28, the results rarely form perfectly isolated subgraphs. As evident, incorrect edges between the line items likely remain. A post-processing step is needed to identify such edges.

Alternatively, when using even-odd line-item predictions, another post-processing step is possible. Since line items are repetitive, an odd line item must always follow an even one and vice versa. Therefore, line items can be identified using a clustering method. By separating each node into two batches - even and odd - and then clustering the resulting nodes based on their top coordinates inside the batches, line items are separable based on the coordinates. The method chosen for the clustering is Density-Based Spatial Clustering of Application with Noise (DBSCAN), with the parameters, $\epsilon = 0.01$ and $\min_samples = 1$.

The resulting binary labels represented with blue and red rectangles for even and odd predictions show a perfect prediction case in Figure 29. The clustering results for even predictions are shown in Figure 18, and in Figure 19 for odd line item predictions.

Figure 18: Clustering Results, Even Line Items, Example 1

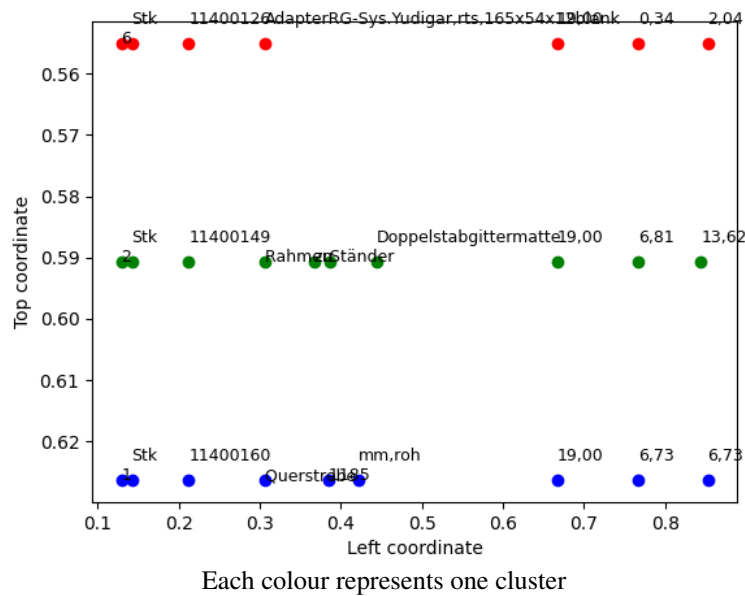
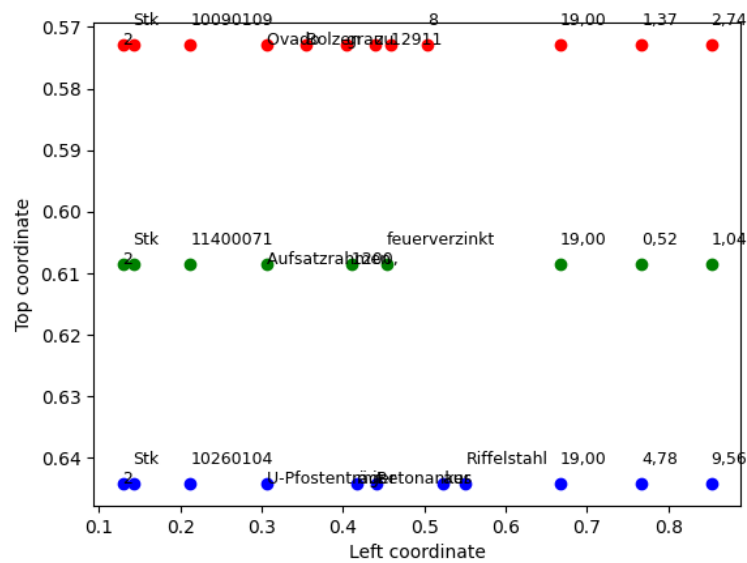


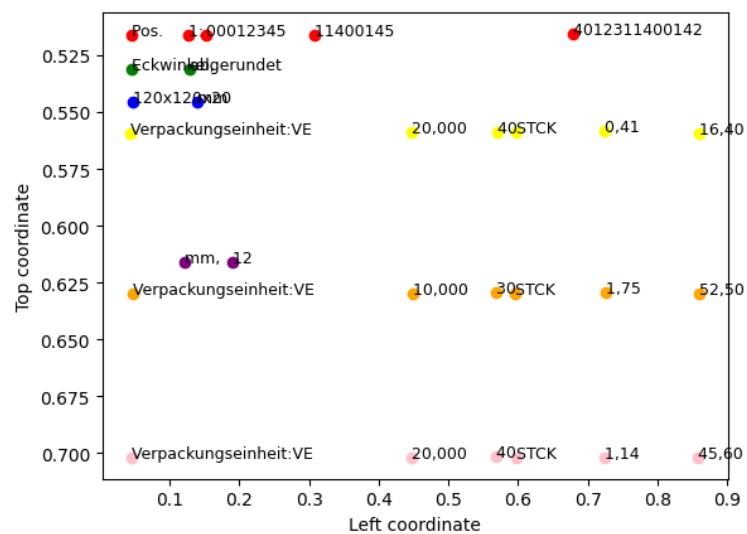
Figure 19: Clustering Results, Odd Line Items, Example 1



Each colour represents one cluster

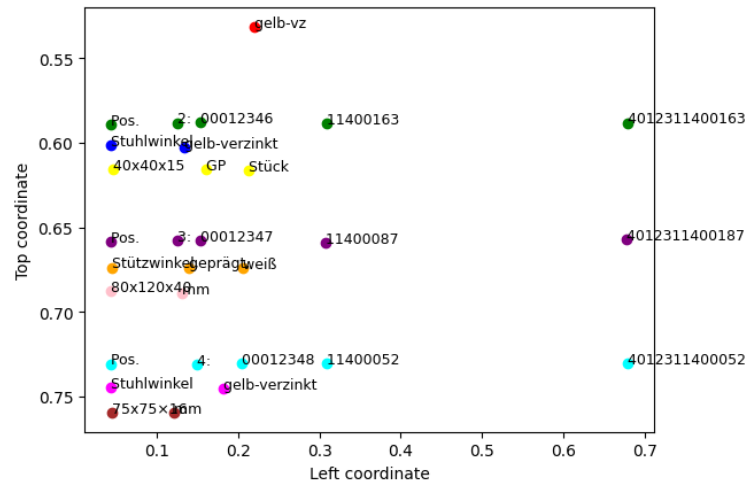
As evident by the clusters, it is generally possible to convert even-odd predictions into separated clusters based on spatial information. Nonetheless, this method fails whenever the initial even-odd predictions fail. For the even-odd predictions shown in Figure 30, the resulting cluster for even predictions, Figure 20, and odd predictions, Figure 21, show that clustering with DBSCAN would create too many incorrect clusters.

Figure 20: Clustering Results, Even Line Items, Example 2



Each colour represents one cluster

Figure 21: Clustering Results, Odd Line Items, Example 2



Each colour represents one cluster

Lastly, the individual models trained could be used in a multi-step pipeline. As the input graph for the node-classification model still contains several edges that incorrectly connect nodes between alternating line items, the link-prediction model could be used to pre-process and prune the document graph. By receiving a document graph as an input, pruning incorrect edges, and only keeping relevant ones before passing the result into the even-odd prediction model, the graph is modified based on the link prediction model before making node-level predictions. Table 11 shows the results of a pipeline approach, using a trained link-prediction model for pruning and an even-odd model for binary classification afterwards. The results indicate that the model does performs worse than the base even-odd models discussed before.

Table 11: Performance, Pipeline approach

Data Used	Accuracy	Micro			Macro		
		F1	Precision	Recall	F1	Precision	Recall
All difficulties	0,5594	0,5594	0,5594	0,5594	0,4464	0,6305	0,5365

The results of the link-prediction model can explain the reason for this performance. Looking at Figure 27, it is evident that even well-performing inference examples can cause issues for later node

classification. The first two line items have two completely isolated subgraphs preventing necessary message passing with relevant information to nodes at the bottom of the table, leading to less meaningful node embeddings. In the current implementation, a pipeline approach is less performant than individual models.

In addition, other trivial post-processing steps are reasonable in the scope of a production environment. As pointed out through the axioms in Chapter 4.1.3.11, line items can never cross each other. This circumstance also infers that tokens that are horizontally aligned can never have a different line item number because otherwise, the axiom would not hold. As shown in Figure 30, some individual node predictions are unreasonable when considering the predictions in the local neighbourhood. For example, the even prediction for token *mm* in the second line item is unreasonable, considering that all other horizontal neighbours are odd predictions. Tokens and their predictions should thus be evaluated after the model’s prediction and checked whether there are any conflicts on a horizontal axis between the line item enumeration. If a conflict of alternating predictions arises, assigning the highest count of line item numbers to the conflicting nodes is reasonable. In addition, the results should also be enriched based on line item metadata about the page. This information could come from an OD model, detecting the count of line items beforehand. By cross-validating the results, incorrect predictions can later be corrected. Independent of the exact pre- or post-processing steps implemented, some form of processing seems reasonable when implementing a graph model for line item predictions in a production environment.

While the task of even-odd and link-prediction was proven to be feasible, it is essential to point out that the most critical node feature with informative value about line items is the node colouring step, explained in Chapter 4.1.3.11. The reasoning behind the feature’s success also highlights one of the main challenges when classifying line item subgraphs structures on a node level. Since line items exist on a global document level above the node level, inferring node-level predictions about these structures is challenging. Even features such as bounding box coordinates do not carry information regarding structures above the node level. This complication is demonstrated through the example prediction task in Figure 12 and Figure 13. Only when considering all bounding box coordinates globally, in Figure 22 and Figure 23, a pattern emerges which is not available to the nodes at the time of message passing. Since one coordinate in the graph might relate to line item 1 in one document

instance and line-item 2 in another, it is non-trivial to assign a line item based on this information confidently. Line item structures appear identifiable when comparing node features globally while looking at the graph as a whole. A complex pre-processing method such as node colouring is necessary to break down this global information onto node-level information, available before the first round of message passing. Because line items inside document graphs are highly isomorphic, it becomes even more challenging to differentiate one from another or by learning node embeddings that could reveal a form of numerical ordering. The link-prediction task likely outperformed the other two since it alleviated the overall burden of inferring the ordering. Even though node labelling boosted the model performance significantly, it is not error-free and likely even provides eventual, incorrect information. As explained, the first axiom explained in Chapter 4.1.3.11 is only correct in about 96% of the cases. Nonetheless, a form of node labelling implemented to capture global subgraph structures as a node-level feature is a reasonable starting point for further research. A potential approach in future research could combine OD models to break down subgraph structures into node features for node classification tasks.

As explained in Chapter 4.1.2, the data was pre-processed to fit the modelling task by removing class imbalances. While this is a crucial step to enable learning in the first place, it does introduce a form of selection bias, as the data used to train the model does not represent the entire document population. Since documents with single line items do frequently occur, there is a need for dealing with such documents. However, introducing single line items into the test data for validation does not alter the performance of any of the three models. Alternatively, the node colouring algorithm can also be used to infer the line item amount directly. Out of all single line item documents available, the node colouring method correctly identified 93,5% of documents. Therefore, the method accurately identifies documents, not incorporating DL. While out of the scope of this thesis, it could also be possible to perform a graph-level prediction that predicts the number of line items prior to any node-level predictions by pooling all graph nodes of the final layer into a graph-level representation.

Lastly, another potential task needs to be mentioned in the scope of this thesis. As proposed in the paper of Wang and Zhang, 2022 and Alsentzer et al., 2020 it is possible to learn subgraph representations of several nodes, similar to representations of a whole graph. A combination of both approaches would first learn subgraph embeddings and then use such embeddings as features for individual nodes

to break down the information of subgraph embeddings to a node level. While the details and the success of such a method are unclear, subgraph embeddings can combine both subgraph and node-level features, potentially bridging the missing informative gap between global subgraph structures and node-level informative features. Subgraph embeddings would likely help the model generate more meaningful higher-dimensional node features rather than a one-dimensional feature vector such as node colouring. In addition, it would tackle the task of multi-node representational learning, explicitly for subgraphs. By doing so, the different structural representations of line items can be evaluated, and possible ways to use a graph model to achieve similar embeddings for identification purposes. However, in this thesis's scope, individual nodes must be classified as part of global subgraphs. Assigning nodes to subgraphs implies that the initial knowledge regarding the subgraph position in the bigger graphs are unavailable, thus not allowing for subgraph representational learning in a production environment.

8 Conclusion

Within the scope of this thesis, three different GCNs were trained to answer the research question: *How can the architecture of Graph Neural Networks be modified to classify line-item subgraph structures inside order documents?*”. The thesis shows that LIR via GCNs is feasible, whereas predicting links between node pairs is more feasible to identify line item structures than to classify nodes directly. Instead of using the final layer to predict integer labels, using node embeddings as input for comparing node similarity improves performance. Independent of the model trained, the node feature choice greatly impacts the model’s performance. The usage of a node labelling method, as introduced by Zhang et al., 2021, Wang and Zhang, 2022, or Zhang and Chen, 2018, is an efficient method for enabling node-level predictions about subgraph structures. While this method boosts the model performance, it also makes the performance dependent on the feature’s existence, as other features did not show a substantial impact. Moreover, the model training did not incorporate other subgraph representations as node features, which could, in theory, enable an even more informative type of learning. In the scope of DU, the thesis contributes to enhancing existing methods of TSR, with line items being the focus. Detecting subgraph structures inside documents by assigning labels to individual nodes is a novel approach worth pursuing, considering the success demonstrated in this work. The concept of node labelling proved to be an essential part of translating global document subgraph structures as a feature for individual nodes. Robust node labelling methods outside the scope of document understanding are an essential feature to enhance node-level representational learning about subgraph structures. While this thesis only dealt with detecting line item subgraph structures, it can be extended to any subgraph structures modelled within graphs. Apart from detecting document subgraph structures, such as headers, address lines, or even complete tables, the prediction task can be applied to different domains outside of DU.

References

- Aiello, M., Monz, C., Todoran, L., Worring, M., et al.** (2002). "Document understanding for a broad class of documents." *International Journal on Document Analysis and Recognition*, 51, 1–16.
- Alsentzer, E., Finlayson, S., Li, M., & Zitnik, M.** (2020). "Subgraph neural networks." *Advances in Neural Information Processing Systems*, 33, 8017–8029.
- Battaglia, P. W., Hamrick, J. B., Bapst, V., Sanchez-Gonzalez, A., Zambaldi, V., Malinowski, M., Tacchetti, A., Raposo, D., Santoro, A., Faulkner, R., et al.** (2018). "Relational inductive biases, deep learning, and graph networks." *arXiv preprint arXiv:1806.01261*.
- Bergstra, J., & Bengio, Y.** (2012). "Random search for hyper-parameter optimization." *Journal of machine learning research*, 132.
- Buckland, M., & Gey, F.** (1994). "The relationship between recall and precision." *Journal of the American society for information science*, 451, 12–19.
- Chen, F., Wang, Y.-C., Wang, B., & Kuo, C.-C. J.** (2020). "Graph representation learning: A survey." *APSIPA Transactions on Signal and Information Processing*, 9, e15.
- Chi, Z., Huang, H., Xu, H.-D., Yu, H., Yin, W., & Mao, X.-L.** (2019). "Complicated table structure recognition." *arXiv preprint arXiv:1908.04729*.
- Costa e Silva, A., Jorge, A. M., & Torgo, L.** (2006). "Design of an end-to-end method to extract information from tables." *International Journal of Document Analysis and Recognition (IJ-DAR)*, 82-3, 144–171.
- Coüasnon, B., & Lemaitre, A.** (2014). "Recognition of tables and forms".
- Defferrard, M., Bresson, X., & Vandergheynst, P.** (2016). "Convolutional neural networks on graphs with fast localized spectral filtering." <http://arxiv.org/pdf/1606.09375v3>
- Devlin, J., Chang, M.-W., Lee, K., & Toutanova, K.** (2018). "Bert: Pre-training of deep bidirectional transformers for language understanding." *arXiv preprint arXiv:1810.04805*.
- Fang, J., Mitra, P., Tang, Z., & Giles, C. L.** (2012). "Table header detection and classification." *Proceedings of the AAAI Conference on Artificial Intelligence*, 261, 599–605.
- Gao, H., Wang, Z., & Ji, S.** (2018). "Large-scale learnable graph convolutional networks." *Proceedings of the 24th ACM SIGKDD international conference on knowledge discovery & data mining*, 1416–1424.

- Girvan, M., & Newman, M. E.** (2002). "Community structure in social and biological networks." *Proceedings of the national academy of sciences*, 99(12), 7821–7826.
- Glorot, X., & Bengio, Y.** (2010). "Understanding the difficulty of training deep feedforward neural networks." *Proceedings of the thirteenth international conference on artificial intelligence and statistics*, 249–256.
- Gori, M., Monfardini, G., & Scarselli, F.** (2005). "A new model for learning in graph domains." *Proceedings. 2005 IEEE International Joint Conference on Neural Networks, 2005.*, 2, 729–734.
- Hagmann, P., Cammoun, L., Gigandet, X., Meuli, R., Honey, C. J., Wedeen, V. J., & Sporns, O.** (2008). "Mapping the structural core of human cerebral cortex." *PLoS biology*, 6(7), e159.
- Hamilton, W., Ying, Z., & Leskovec, J.** (2017). "Inductive representation learning on large graphs." *Advances in neural information processing systems*, 30.
- Holeček, M., Hoskovec, A., Baudiš, P., & Klinger, P.** (2019). "Table understanding in structured documents." *abs 1804.6236*, 158–164. <https://doi.org/10.1109/ICDARW.2019.40098>
- Kasiviswanathan, S. P., Nissim, K., Raskhodnikova, S., & Smith, A.** (2013). "Analyzing graphs with node differential privacy." *Theory of Cryptography: 10th Theory of Cryptography Conference, TCC 2013, Tokyo, Japan, March 3-6, 2013. Proceedings*, 457–476.
- Kearnes, S., McCloskey, K., Berndl, M., Pande, V., & Riley, P.** (2016). "Molecular graph convolutions: Moving beyond fingerprints." *Journal of computer-aided molecular design*, 30, 595–608.
- Kipf, T. N., & Welling, M.** (2016). "Semi-supervised classification with graph convolutional networks." *arXiv preprint arXiv:1609.02907*.
- Kleinberg, J. M.** (1999). "Authoritative sources in a hyperlinked environment." *Journal of the ACM (JACM)*, 46(5), 604–632.
- Krogh, A., & Hertz, J.** (1991). "A simple weight decay can improve generalization." *Advances in neural information processing systems*, 4.
- Li, P., Wang, Y., Wang, H., & Leskovec, J.** (2020). "Distance encoding: Design provably more powerful neural networks for graph representation learning." *Advances in Neural Information Processing Systems*, 33, 4465–4478.

- Li, Y., Yu, R., Shahabi, C., & Liu, Y.** (2017). "Diffusion convolutional recurrent neural network: Data-driven traffic forecasting." *arXiv preprint arXiv:1707.01926*.
- Lohani, D., Belaid, A., & Belaid, Y.** (2019). "An invoice reading system using a graph convolutional network." *Asian Conference on Computer Vision*, 144–158.
- Majeed, A., & Rauf, I.** (2020). "Graph theory: A comprehensive survey about graph theory applications in computer science and social networks." *Inventions*, 51, 10. <https://doi.org/10.3390/inventions5010010>
- McKay, B. D., et al.** (1981). "Practical graph isomorphism."
- Monti, F., Boscaini, D., Masci, J., Rodola, E., Svoboda, J., & Bronstein, M. M.** (2017). "Geometric deep learning on graphs and manifolds using mixture model cnns." *Proceedings of the IEEE conference on computer vision and pattern recognition*, 5115–5124.
- Newman, M. E.** (2003). "The structure and function of complex networks." *SIAM review*, 452, 167–256.
- Pascanu, R., Mikolov, T., & Bengio, Y.** (2013). "On the difficulty of training recurrent neural networks." *International conference on machine learning*, 1310–1318.
- Prasad, D., Gadpal, A., Kapadni, K., Visave, M., & Sultanpure, K.** (2020). "Cascadetabnet: An approach for end to end table detection and structure recognition from image-based documents." *Proceedings of the IEEE/CVF conference on computer vision and pattern recognition workshops*, 572–573.
- Qasim, S. R., Mahmood, H., & Shafait, F.** (2019). "Rethinking table recognition using graph neural networks." *2019 International Conference on Document Analysis and Recognition (ICDAR)*, 142–147.
- Riba, P., Dutta, A., Goldmann, L., Fornés, A., Ramos, O., & Lladós, J.** (2019). "Table detection in invoice documents by graph neural networks." *2019 International Conference on Document Analysis and Recognition (ICDAR)*, 122–127.
- Scarselli, F., Gori, M., Tsoi, A. C., Hagenbuchner, M., & Monfardini, G.** (2008). "The graph neural network model." *IEEE transactions on neural networks*, 201, 61–80.

- Schreiber, S., Agne, S., Wolf, I., Dengel, A., & Ahmed, S.** (2017). "Deepdesrt: Deep learning for detection and structure recognition of tables in document images." *2017 14th IAPR international conference on document analysis and recognition (ICDAR)*, 1, 1162–1167.
- Shafait, F., & Smith, R.** (2010). "Table detection in heterogeneous documents." *Proceedings of the 9th IAPR International Workshop on Document Analysis Systems*, 65–72.
- Šimsa, Š., Šulc, M., Uříčář, M., Patel, Y., Hamdi, A., Kocián, M., Skalický, M., Matas, J., Doucet, A., Coustaty, M., et al.** (2023). "Docile benchmark for document information localization and extraction." *arXiv preprint arXiv:2302.05658*.
- Singh, H., & Sharma, R.** (2012). "Role of adjacency matrix & adjacency list in graph theory." *International Journal of Computers & Technology*, 31, 179–183.
- Smith, R.** (2007). "An overview of the tesseract ocr engine." *Ninth international conference on document analysis and recognition (ICDAR 2007)*, 2, 629–633.
- Smock, B., Pesala, R., & Abraham, R.** (2022). "Pubtables-1m: Towards comprehensive table extraction from unstructured documents." *Proceedings of the IEEE/CVF Conference on Computer Vision and Pattern Recognition*, 4634–4642.
- Srivastava, N., Hinton, G., Krizhevsky, A., Sutskever, I., & Salakhutdinov, R.** (2014). "Dropout: A simple way to prevent neural networks from overfitting." *The journal of machine learning research*, 151, 1929–1958.
- Vashisth, S., Mullen, A., Emmott, S., & Lozada, A.** (2022). "Market guide for intelligent document processing solutions."
- Veličković, P., Cucurull, G., Casanova, A., Romero, A., Lio, P., & Bengio, Y.** (2017). "Graph attention networks." *arXiv preprint arXiv:1710.10903*.
- Vinyals, O., Bengio, S., & Kudlur, M.** (2015). "Order matters: Sequence to sequence for sets." *arXiv preprint arXiv:1511.06391*.
- Wang, X., & Zhang, M.** (2022). "Glass: Gnn with labeling tricks for subgraph representation learning." *International Conference on Learning Representations*.
- Wu, Z., Pan, S., Chen, F., Long, G., Zhang, C., & Philip, S. Y.** (2020). "A comprehensive survey on graph neural networks." *IEEE transactions on neural networks and learning systems*, 321, 4–24.

- Yao, L., Mao, C., & Luo, Y.** (2019). "Graph convolutional networks for text classification." *Proceedings of the AAAI conference on artificial intelligence*, 3301, 7370–7377.
- Ying, R., He, R., Chen, K., Eksombatchai, P., Hamilton, W. L., & Leskovec, J.** (2018). "Graph convolutional neural networks for web-scale recommender systems." *Proceedings of the 24th ACM SIGKDD international conference on knowledge discovery & data mining*, 974–983.
- You, J., Gomes-Selman, J. M., Ying, R., & Leskovec, J.** (2021). "Identity-aware graph neural networks." *Proceedings of the AAAI conference on artificial intelligence*, 3512, 10737–10745.
- Zhang, M., & Chen, Y.** (2018). "Link prediction based on graph neural networks." *Advances in neural information processing systems*, 31.
- Zhang, M., Li, P., Xia, Y., Wang, K., & Jin, L.** (2021). "Labeling trick: A theory of using graph neural networks for multi-node representation learning." *Advances in Neural Information Processing Systems*, 34, 9061–9073.

Appendix

Table 12: Tuning Results, Straight-odd Prediction

K	BS¹	Layers	Dropout	HN²	LR³	WD⁴	Acc.⁵	Mac. F1⁶	Mic. F1⁷
4	32	3	0.3	512	0.0001	0.001	0,7988	0,7986	0,7988
3	16	3	0.3	512	0.00001	0.001	0,7947	0,7947	0,7947
3	16	4	0.5	256	0.00001	0.001	0,7936	0,7933	0,7936
3	16	4	0.7	256	0.0001	0.001	0,7934	0,7933	0,7934
3	16	3	0.7	1024	0.00001	0.001	0,7920	0,7920	0,7920
4	32	2	0.7	1024	0.00001	0.001	0,7916	0,7915	0,7916
3	16	4	0.5	256	0.0001	0.01	0,7886	0,7878	0,7886
2	16	2	0.5	256	0.0001	0.001	0,7878	0,7877	0,7878
3	16	4	0.3	1024	0.00001	0.01	0,7863	0,7862	0,7863
4	16	4	0.5	1024	0.00001	0.01	0,7854	0,7819	0,7854
2	64	3	0.7	512	0.00001	0.001	0,7830	0,7830	0,7830
2	16	3	0.5	256	0.000001	0.01	0,7826	0,7824	0,7826
3	64	2	0.3	512	0.000001	0.01	0,7825	0,7823	0,7825
2	32	2	0.3	256	0.000001	0.01	0,7823	0,7822	0,7823
3	32	3	0.3	256	0.000001	0.01	0,7821	0,7819	0,7821
2	32	4	0.7	1024	0.000001	0.001	0,7817	0,7814	0,7817
2	64	2	0.3	512	0.000001	0.01	0,7806	0,7804	0,7806
2	64	2	0.7	512	0.000001	0.001	0,7796	0,7796	0,7796
2	16	3	0.3	512	0.000001	0.001	0,7792	0,7783	0,7792
4	16	2	0.7	512	0.000001	0.01	0,7792	0,7792	0,7792
2	64	4	0.7	512	0.00001	0.01	0,7788	0,7783	0,7788
2	16	3	0.7	1024	0.00001	0.01	0,7745	0,7734	0,7745
2	16	2	0.7	256	0.00001	0.01	0,7726	0,7725	0,7726

continued

Table 12: Tuning Results, Straight-odd Prediction

K	BS¹	Layers	Dropout	HN²	LR³	WD⁴	Acc.⁵	Mac. F1⁶	Mic. F1⁷
2	16	3	0.7	512	0.0001	0.01	0,7607	0,7577	0,7607
4	16	4	0.7	512	0.000001	0.01	0,7595	0,7595	0,7595
2	64	2	0.7	256	0.000001	0.01	0,5379	0,3835	0,5379
4	64	2	0.7	512	0.000001	0.001	0,5285	0,3468	0,5285
3	16	3	0.7	512	0.000001	0.001	0,5283	0,3459	0,5283

¹ Batch Size;

² Hidden Neurons;

³ Learning Rate;

⁴ Weight Decay;

⁵ Validation Accuracy;

⁶ Validation Macro F1;

⁷ Validation Micro F1

All performance values are rounded to four decimal places

Table 13: Tuning Results, Link Prediction

K	BS¹	Layers	Dropout	HN²	LR³	WD⁴	Acc.⁵	Mac. F1⁶	Mic. F1⁷
2	32	3	0.3	1024	0.00001	0.001	0,9038	0,8916	0,9038
2	16	2	0.7	256	0.0001	0.001	0,9034	0,8912	0,9034
4	16	2	0.7	1024	0.00001	0.001	0,9034	0,8909	0,9034
3	16	3	0.5	512	0.0001	0.001	0,9033	0,8910	0,9033
2	32	3	0.5	1024	0.00001	0.01	0,9031	0,8907	0,9031
3	32	4	0.3	256	0.00001	0.01	0,9031	0,8904	0,9031

continued

Table 13: Tuning Results, Link Prediction

K	BS¹	Layers	Dropout	HN²	LR³	WD⁴	Acc.⁵	Mac. F1⁶	Mic. F1⁷
2	32	4	0.3	256	0.00001	0.001	0,9030	0,8905	0,9030
2	16	2	0.3	256	0.0001	0.01	0,9025	0,8902	0,9025
2	16	2	0.7	1024	0.0001	0.001	0,9024	0,8903	0,9024
3	32	4	0.3	512	0.0001	0.001	0,9020	0,8899	0,9020
3	64	2	0.7	512	0.0001	0.01	0,9016	0,8884	0,9016
4	16	3	0.5	256	0.00001	0.001	0,9016	0,8885	0,9016
3	64	4	0.5	256	0.00001	0.001	0,9014	0,8882	0,9014
3	32	3	0.7	256	0.00001	0.01	0,8995	0,8867	0,8995
2	64	3	0.3	1024	0.000001	0.001	0,8980	0,8846	0,8980
3	32	3	0.3	1024	0.000001	0.001	0,8971	0,8838	0,8971
2	16	2	0.3	512	0.000001	0.001	0,8955	0,8822	0,8955
4	32	2	0.3	1024	0.000001	0.001	0,8945	0,8806	0,8945
4	64	3	0.5	1024	0.0001	0.01	0,8939	0,8791	0,8939
2	16	3	0.5	1024	0.000001	0.001	0,8923	0,8787	0,8923
2	64	3	0.3	512	0.000001	0.01	0,8901	0,8740	0,8901
4	32	4	0.3	1024	0.000001	0.001	0,8585	0,8330	0,8585
3	64	3	0.5	512	0.000001	0.01	0,7591	0,6889	0,7591
4	32	4	0.3	256	0.000001	0.01	0,7117	0,6028	0,7117
3	64	4	0.5	256	0.000001	0.01	0,6369	0,3911	0,6369
3	32	4	0.7	1024	0.000001	0.001	0,6213	0,4250	0,6213

continued

Table 13: Tuning Results, Link Prediction

K	BS¹	Layers	Dropout	HN²	LR³	WD⁴	Acc.⁵	Mac. F1⁶	Mic. F1⁷
----------	-----------------------	---------------	----------------	-----------------------	-----------------------	-----------------------	-------------------------	----------------------------	----------------------------

¹ Batch Size;

² Hidden Neurons;

³ Learning Rate;

⁴ Weight Decay;


⁵ Validation Accuracy;

⁶ Validation Macro F1;

⁷ Validation Micro F1

All performance values are rounded to four decimal places

Figure 22: Example Document of left token



Garbor Aktiengesellschaft

Garbor AG, Bahnhofstraße 27, 33602 Bielefeld

Bestellung

Workist GmbH
 Linienstr. 126
 10115 Berlin
 Deutschland

Datum: 23.05.22
 Bestellnr.: 42232214
 Ansprechpartner: Heiko Schmidt
 Telefon : +49 2078330143
 Email: hschmidt@garbor-ag.de

Wir bestellen hiermit die folgenden Artikel:

Pos.	Artikelbeschreibung, -Nr.	Menge	Preis/Stk	Gesamt
1	Sechskantenschraub DIN 934 M8x16 A4-70 Art. Nr. 1400067	100 Stk	0,52	5,20
2	Kastenschloss Jäger 2-auntore, 1 Zvz, 118x100 Art. Nr. 10050050	1 Stk	0,94	0,94
3	Hakenkappe Art. Nr. 10050113	100 Stk	0,94	9,40
4	Haltebock H 2 H 2 Seilabermatten V 2 Art. Nr. 1400001	1 Stk	0,73	0,73
5	Rahmen H 14 Schlechtspannabst	1 Stk	1,97	1,97
6	Distanzstueck Schwerlastregal 250,10ervz Art. Nr. 1400033	1 Stk	1,79	1,79
7	Aufhängemaß Schallfenster H 145 Art. Nr. 1400054	1 Stk	0,94	0,94
8	U-Bogen 100x20x10 Rohr 1,5mm Art. Nr. 1400108	100 Stk	2,30	230,00
9	FLK 11 Art. Nr. 10000000	1 Stk	0,97	0,97
10	Dielenleiste Art. Nr. 1400739	1 Stk	1,40	1,40
Warenwert				226,30
				EUR
Total				226,30
				EUR

Lieferadresse:

Garbor AG
 Bahnhofstraße 45
 33602 Bielefeld

Lieferdatum: SOFORT

Garbor AG
 Bahnhofstraße 27
 33602 Bielefeld
 Tel.: +49 2078330143
 Email: info@garbor-ag.de
 www.garbor-ag.de

Bankverbindung
 IBAN : DE41 1000 5467 78 67
 BIC: SPBI DE33 XXX4

Geschäftsführer: Dr. Paul Wagner
 Handelsregister: HRB 3215013 D
 Registergericht: Amtsgericht Bielefeld

Red rectangles indicate bounding boxes around tokens

Green rectangles indicate bounding boxes around line items

Figure 23: Example Document of right token



Brasius

Bestellung

123456678990 /

/ 08.08.2020


Seite: 2

Artikel	Menge	Einheit	Preis	Gesamt EUR
Übertrag:				114,50
Verpackungseinheit VE	50,000	50 STCK	0,23	11,50
Pos. 8: 100054324 10020073			4012310020073	
Verstellwinkel, weiß 65x80x20 mm				
Verpackungseinheit VE	50,000	50 STCK	0,64	32,00
Pos. 6: 100054322 10070040			4012310070040	
Kistenverschluss mit Haken 49x19 mm, gbvz				
Verpackungseinheit VE	10,000	20 STCK	1,24	24,40
Pos. 7: 100054323 11400012			4012311400012	
Küchenfahnenessen, gbvz 19x64 mm, SD 1/8				
Verpackungseinheit VE	5,000	16 STCK	0,86	8,90
Pos. 8: 100054324 11400044			4012311400044	
Sturmhaken mit Oberlaufplatte 120x50 mm, gbvz				
Verpackungseinheit VE	6,000	8 STCK	1,40	8,38
Pos. 9: 100054325 11400046			4004311400046	
Oberlaufplatte, gbvz 67x37 mm				
Verpackungseinheit VE	25,000	25 STCK	0,42	10,50
Pos. 10: 100054326 10133016			4012310133016	
Lochband, gebz.vz 17 mm, 16 H				
Verpackungseinheit VE	5,000	8 STCK	5,20	26,30
Pos. 11: 100054327 10020072			4012310020072	
Lochband, vz, weiß				
Übertrag:				232,58

Red rectangles indicate bounding boxes around tokens


Green rectangles indicate bounding boxes around line items

Figure 24: Easy document graph



BAE & Co. KG, Laternenweg 12, 45721 Haltern am See

Workist GmbH
Linienstr. 126
10115 Berlin
Germany



Lieferanschrift:
BAE & Co. KG
Laternenweg 14
45721 Haltern am See
Tel: 01234/654-0865

Rechnungsanschrift:
BAE & Co. KG
Laternenweg 12
45721 Haltern am See
Tel: 43210/654-9851

Kundennr.: 19940672
Bearbeiter: Bjarne Rittenfeld
Bestell-Nr.: NSE987654
Datum: 01.03.2021

Seite 1

Bestellung

hiermit bestellen wir folgende Positionen:

Menge	Art.-Nr.	Bezeichnung	USt.	E-Preis	G-Preis
1	11490129	Adapter RC Sys. Yubaer, 165x54x12, blank	19,00	5,84	6,94
1	10030103	Overst. Bolzen Head, 120, 1/8"	19,00	8,97	10,77
1	11490143	Rahmen, 1/2" Stand, Doppel, 1/2" Baillermatt	19,00	5,84	6,94
1	11490071	Aufsatzrahmen, 1/2" Stand, 1/2" Baillermatt	19,00	5,84	6,94
1	11490160	Querschub, 1/2" Stand, 1/2" Baillermatt	19,00	5,84	6,94
1	10200104	U-Flachenträger, 1/2" Stand, 1/2" Baillermatt	19,00	5,84	6,94

Gesamt Netto (19%): 35,73 EUR

19% USt.: 6,72 EUR

Gesamt: 42,09 EUR**Lieferdatum: 24.07.2022**

Unsere USt-IdNr. DE123456789

Wir danken für eine schnellstmögliche Abwicklung.



Bankverbindung: Deutsche Bank

BLZ: 123 456 79

KTO: 123456

Ust-ID: DE123456789

Red rectangles indicate bounding boxes around tokens

Green rectangles indicate bounding boxes around line items

Figure 25: Medium document graph

Auftrag
** Sortimentsbestellung **

Lieferant WORKIST GMBH C/O DB MINDBOX HOLZMARKTSTRASSE 6-9 10179 BERLIN GERMANY	Lieferanschrift BAE&Co. KG Laternenweg 14 45721 Haltern am See 01234/654-0865	Rechnungsanschrift BAE&Co. KG Laternenweg 12 4712 Haltern am See
	Liefertag Incoterms Disponent Der Liefertermin gilt für Warenlieferung in unsere Niederlassung	08.07.2020 ABC dhg83a Datum Auftrag Auftragsdatum Seite Projekt Nr.
		01.07.2020 3845198/4466 01.07.2020 1

Warennummer.	WGR.	Text	Kolli	Stück	Einheit	Bezugspreis
9999910000100 K31SRV	1400100	SLANGKOPPLING 1/2" 1/2"	10	100	Stk	0,00EUR
9999910000100 K31SRV	1400100	DAMMITZUGSLANG 1/2" 1/2"	10	100	Stk	0,00EUR
9999910000100 K31SRV	1020073	DAMMITZUGSLANG 1/2" 1/2"	10	100	Stk	0,00EUR
9999910000100 K31SRV	1090012	SLICKKOPPLING 1/2" 1/2"	10	100	Stk	0,00EUR
9999910000100 K31SRV	1000000	SLICKSLANGSTOPF 1/2" 1/2"	10	100	Stk	0,00EUR
9999910000100 K31SRV	1020073	SLICKSLANGSTOPF 1/2" 1/2"	10	100	Stk	0,00EUR
9999910000100 K31SRV	1400044	SLICK APPARATKOPPLING 1/2" 1/2"	10	100	Stk	0,00EUR
9999910000100 K31SRV	1400177	SLICK APPARATKOPPLING 1/2" 1/2"	10	100	Stk	0,00EUR

Red rectangles indicate bounding boxes around tokens

Green rectangles indicate bounding boxes around line items

Figure 26: Hard document graph

BRASIUS
GMBH

Bestellung

123456678990 / / 08.08.2020 Seite: 2

Artikel	Menge	Einheit	Preis	Gesamt EUR
Übertrag:				114,50
Verpackungseinheit VE	50,000	50 STCK	0,23	11,50
Pos. 100054324 10020072 4012310020072				
Verstellwinkel weiß 65x80x20 mm				
Verpackungseinheit VE	50,000	50 STCK	0,56	28,00
Pos. 100054322 10070040 4012310070040				
Kistenverschluss mit Haken 49x49 mm glbz				
Verpackungseinheit VE	10,000	20 STCK	1,22	24,40
Pos. 100054323 11400012 4012311400012				
Kuchenzahmenset glbz 19x60 mm 50/50				
Verpackungseinheit VE	5,000	10 STCK	0,60	3,00
Pos. 100054324 11400044 4012311400044				
Stumpfhaken mit Ober- und Unterplatte 120x50 mm glbz				
Verpackungseinheit VE	6,000	6 STCK	1,38	8,38
Pos. 100054325 11400040 4004311400040				
Ober- und Unterplatte glbz 37x37 mm				
Verpackungseinheit VE	25,000	25 STCK	0,42	10,50
Pos. 100054326 10133016 4012310133016				
Lochband serbz.vz 15 mm 100 m				
Verpackungseinheit VE	5,000	5 STCK	5,20	26,00
Pos. 100054327 10020072 4012310020072				
Lochband vz.weiß				
Übertrag:				232,58


Red rectangles indicate bounding boxes around tokens

Green rectangles indicate bounding boxes around line items

BRASIUS
www.brasius.eu

Red rectangles indicate bounding boxes around tokens
Green rectangles indicate bounding boxes around line items

Figure 28: Link prediction inference, Example 2


Brasius

Brasius GmbH | Hermelinger Weg 34-36 | D-47433 Kleve

Workist GmbH
c/o DB mindbox
Holzmarktstraße 6-9

D-10179 Berlin

Telefon: 01234-1234
Telefax: 01234-1235

Bestellung

Beleg-Nr.: 123456678990

Datum: 08.08.2020

Sachbearbeiter: 123 Meier, Stefan


Seite: 1

Artikel	Menge	Einheit	Preis	Gesamt EUR
<p>Lieferanschrift: Firma Brasius GmbH Hermelinger Weg 36 47533 Kleve</p> <p>Geschäftsart: Lager Lieferdatum: 12.08.2020</p>				
<p>Pos: 1 00012345 11400143 4012311400142</p> <p>Eckwinkel abgerundet gelb-vz</p> <p>120x120x20 mm</p> <p>Verpackungseinheit VL</p>	20.000	16 STCK	0,4	16,40
<p>Pos: 2 00012346 11400163 4012311400163</p> <p>Stuhlwinkel gelb verzinkt</p> <p>40x40x13 mm, CN 12 Stück</p> <p>Verpackungseinheit VL</p>	40.000	36 STCK	1,75	52,50
<p>Pos: 3 00012347 11400087 4012311400187</p> <p>Stützwinkel gepreßt weiß</p> <p>80x120x40 mm</p> <p>Verpackungseinheit VL</p>	20.000	40 STCK	1,14	45,60
<p>Pos: 4 00012348 11400052 4012311400052</p> <p>Stuhlwinkel gelb verzinkt</p> <p>75x75x10 mm</p>				
Übertrag:				114,50

Red rectangles indicate bounding boxes around tokens


Green rectangles indicate bounding boxes around line items

Figure 29: Even-odd inference, Example 1



BAE & Co. KG, Laternenweg 12, 45721 Haltern am See

Workist GmbH
Linienstr. 126
10115 Berlin
Germany



Lieferanschrift:
BAE & Co. KG
Laternenweg 14
45721 Haltern am See
Tel: 01234/654-0865

Rechnungsanschrift:
BAE & Co. KG
Laternenweg 12
45721 Haltern am See
Tel: 43210/654-9851

Kundennr.: 19940672

Bearbeiter: Bjarne Rittenfeld

Bestell-Nr.: NSE987654

Datum: 01.03.2021

Seite 1

Bestellung

hiermit bestellen wir folgende Positionen:

Menge	Art.-Nr.	Bezeichnung	USt.	E-Preis	G-Preis
1 Stk	11400126	AdapterRG-Sys.Yudicor.rts.165x54x12blank	19,00	0,84	2,04
1 Stk	10090109	Overd.Bolzen brau 12911	19,00	1,37	2,74
1 Stk	11400149	Rahmenku Standel Doppelstabgittermatte	19,00	6,81	13,62
1 Stk	11400071	Aufsatzrahmen 1200 feuerverzinkt	19,00	0,52	1,04
1 Stk	11400160	Querstrebe 1185 mm roh xvw	19,00	6,73	6,73
1 Stk	10260104	U-Postenträger mit Betonanker aus Riffelstahl	19,00	4,78	9,56

Gesamt Netto (19%): 35,73 EUR

19% USt.: 6,72 EUR

Gesamt: 42,09 EUR**Lieferdatum: 24.07.2022**

Unsere USt-IdNr. DE123456789

Wir danken für eine schnellstmögliche Abwicklung.



Bankverbindung: Deutsche Bank

BLZ: 123 456 79


KTO: 123456

Ust-ID: DE123456789

Red and blue rectangles indicate even and odd predictions

Green rectangles indicate bounding boxes around line items

Figure 30: Even-odd inference, Example 2


Brasius

Brasius GmbH | Hermelinger Weg 34-36 | D-47433 Kleve

Workist GmbH
c/o DB mindbox
Holzmarktstraße 6-9

D-10179 Berlin

Telefon: 01234-1234
Telefax: 01234-1235

Bestellung

Beleg-Nr.: 123456678990

Datum: 08.08.2020

Sachbearbeiter: 123 Meier, Stefan

Seite: 1

Artikel	Menge	Einheit	Preis	Gesamt EUR
Lieferanschrift: Firma Brasius GmbH Hermelinger Weg 36 47533 Kleve				
Geschäftsart: Lager Lieferdatum: 12.08.2020				
Pos 1: 00012345 11400145 4012311400142 Eckwinkel abgerundet gelb-vz 120x120x20 mm Verpackungseinheit VE	20.000	40 STÜCK	0,41	16,40
Pos 2: 00012346 11400163 4012311400163 Stuhlwinkel gelb-verzinkt 40x40x15 mm GR 12 Stück Verpackungseinheit VE	10.000	30 STÜCK	1,75	52,50
Pos 3: 00012347 11400087 4012311400187 Stützwinkel geprägt weiß 80x120x40 mm Verpackungseinheit VE	20.000	40 STÜCK	1,14	45,60
Pos 4: 00012348 11400052 4012311400052 Stuhlwinkel gelb-verzinkt 75x75x16 mm				
Übertrag:				114,50

Red and blue rectangles indicate even and odd predictions
 Green rectangles indicate bounding boxes around line items